The production and consumption of extracellular polymeric substances in an intertidal diatom mat

Tanja C.W. Moerdijk-Poortvliet[1,2], Olivier Beauchard[1,4,5], Lucas J. Stal[1,3], Henricus T.S. Boschker[1]

[1]NIOZ Royal Institute for Sea Research and Utrecht University, PO Box 140, 4401 AC Yerseke, The Netherlands.

[2]HZ University of Applied Sciences, Chemistry Department, PO Box 364, 4380 AJ Vlissingen, the Netherlands

[3]University of Amsterdam, Department of Freshwater and Marine Ecology, PO Box 94248, 1090 GE Amsterdam, The Netherlands

[4]Flanders Marine Institute (VLIZ), InnovOcean site, Wandelaarkaai 7, 8400 Oostende, Belgium

[5]University of Antwerp, Department of Biology, Ecosystem Management Research Group (ECOBE), Universiteitsplein 1, 2610 Antwerpen, Belgium

*Corresponding author: T.C.W. Moerdijk-Poortvliet, Royal Netherlands Institute for Sea Research (NIOZ), P.O. Box 140, 4400 AC Yerseke, The Netherlands.

E-mail: tanja.moerdijk@gmail.com

Phone: +31 113577300

Fax: +31 113573616

Running head: The production and consumption of EPS

ABSTRACT: The seasonal changes in the production of extracellular polymeric substances (EPS) and short chain organic acids (SCOA) exuded by benthic diatoms and the use of these exudates as a carbon source by heterotrophic bacteria were investigated. An *in-situ* ^{13}C pulse-chase method was used to follow the fate of EPS for 5 consecutive days. These experiments were done at 2-month intervals for one year. The EPS were recovered from the sediment as two operational defined fractions (i.e. water-extractable and EDTA-extractable EPS). The seasonal differences of EPS production correlated to light intensity and temperature. From February until June the biomass and production of diatoms and bacteria were closely coupled. It was concluded that SCOA were the most important substrates for the bacteria. Especially sulfate-reducing bacteria (SRB) benefited from SCOA released by diatoms. From August on, the coupling of biomass and production of diatoms and bacteria became less strong and was almost lost in December. During the period of August until December, EPS produced by diatoms promoted the growth of other bacterial taxa rather than SRB, and the production of SCOA was low. The seasonal variation in exudates produced by diatoms therefore played an important role in shaping the community composition and maintaining the diversity of the associated bacteria.

KEY WORDS: microphytobenthos, in-situ ^{13}C-labeling, extracellular polymeric substances

INTRODUCTION

Intertidal sediments support extensive and diverse populations of microorganisms, which develop complex microbial communities. In temperate regions, benthic diatoms are the dominant organisms of the microphytobenthic communities and the biofilms they produce color the sediment surface brown. The diatoms contribute a major part of the total autotrophic production in these intertidal benthic ecosystems (Admiraal et al. 1984, MacIntyre & Cullen 1996, Underwood and Kromkamp 1999). These benthic diatom mats exhibit high rates of photosynthesis and a substantial proportion of the inorganic carbon they fix may be exuded into the environment as extracellular polymeric substances (EPS) or short chain organic acids (SCOA) (Underwood & Paterson 2003, Miyatake et al. 2014). In addition to direct release by diatoms, SCOA may also be produced as fermentation products during the anaerobic degradation of diatom EPS (McKew et al. 2013). EPS- and SCOA-releasing diatoms stimulate bacterial growth and the great variety of substrates could play a role in generating and maintaining bacterial diversity (Amin et al. 2012).

EPS are exuded through various mechanisms and play an important role in the ecology of diatom mats (Edgar & Pickett-Heaps 1984). For instance, EPS exudation allows motility of diatoms, which is crucial for epipelic species because it enables them to migrate into the sediment when the tide comes in, preventing them from being grazed, as well as providing them access to nutrients (Consalvey et al. 2004). Furthermore, EPS are sometimes produced as the result of unbalanced growth, i.e. growth that does not lead to proportional synthesis of the cell's structural components because the essential nutrients (e.g. nitrogen, phosphorus, sulfur and iron) are lacking or limiting and components are synthesized that lack these nutrients (e.g. carbohydrates and lipids)) (Stal 2010). Because the cell's storage capacity is limited, excess fixed carbon is exuded as EPS. After exudation, EPS accumulate in the surficial sediments where they become available for heterotrophic bacteria, or are washed away during tidal immersion, and/or become part of the biofilm matrix (Yallop et al. 1994, Stal 2010,

68 Taylor et al. 2013). EPS comprise either low-molecular dissolved compounds or consist of more
69 complex colloidal or gel-like material, such as mucilage. The diatoms, the mucilage, and the sediment
70 produce a coherent structure - the biofilm or mat - that stabilizes the sediment surface and avoids re-
71 suspension of the diatoms. EPS may further serve to protect the diatoms from environmental stress,
72 such as changes in temperature, salinity, nutrient availability, desiccation and UV radiation (Hoagland
73 et al. 1993, Underwood & Paterson 2003). Last but not least, EPS provide a carbon source to the
74 benthic food web, which includes heterotrophic bacteria (Middelburg et al. 2000).
75
76 The EPS formation by benthic diatoms has been extensively studied. However, thus far most studies
77 were done in pure cultures and/or focused on the measurement of the content of EPS fractions thereby
78 neglecting effects of community interactions, production and turnover rates of these exudates (Smith
79 & Underwood 1998, Pierre et al. 2014). Most research has been carried out on the dominant
80 carbohydrate component of these exudates, which is undoubtedly important in sediment carbon
81 cycling (Bellinger et al. 2009, Oakes et al. 2010, Taylor et al. 2013). However, EPS may also contain
82 proteins, lipids, nucleic acids and other biopolymers such as humic substances (Flemming &
83 Wingender 2010). Carbohydrates are known to be major intermediates in the rapid transfer of carbon
84 between diatoms and heterotrophic bacteria (Middelburg et al. 2000, Evrard et al. 2008, Bellinger et
85 al. 2009, Taylor et al. 2013). Besides gaining knowledge on EPS dynamics, understanding interactions
86 between diatoms and heterotrophic bacteria is important as they modify each other's behavior and
87 eventually impact biogeochemical cycles (Bruckner et al. 2011, Amin et al. 2012).
88
89 The research question of this exploratory study was how carbon, which originated from EPS and
90 SCOA produced by diatoms, flows to the heterotrophic bacterial community in an intertidal mudflat
91 and how this flow changes seasonally. By using an in-situ ^{13}C pulse-chase method (Middelburg et al.
92 2000) in combination with liquid chromatography isotope ratio mass spectrometry (LC/IRMS) it was

possible to follow the fate of the applied ^{13}C label from carbon fixation to EPS and SCOA exudation (Moerdijk-Poortvliet et al. 2014, 2017). Here, using the same experiment of Moerdijk-Poortvliet et al. (2017), we followed the fate of the applied ^{13}C label to the heterotrophic bacteria. Phospholipid-derived fatty acid (PLFA) biomarker analysis was used to differentiate between benthic diatoms and different groups of heterotrophic bacteria.

MATERIALS AND METHODS

Study site and in situ ^{13}C labeling experiments

In 2011, in-situ ^{13}C-labeling experiments were carried out at approximately 2-months intervals at the Zandkreek intertidal mudflat, which is situated along the southern shore of the Oosterschelde estuary in the southwest of the Netherlands (51°32'41"N, 3°53'22"E). The sampling site was located 0.15 m below the mean tidal level and the emersion period was approximately 6 h per tidal cycle. Bioturbating fauna such as the amphipod crustacean *Corophium volutator* and the hydrobiid snail *Peringia ulvae* became active starting late spring (June) gaining higher grazing rates mixing the sediment top layer during summer. Detailed information on the study site and its sampling is found in Moerdijk-Poortvliet et al. (2017).

Experiments started immediately after emersion of the mudflat. Two 500×500 mm stainless steel frames were pushed into the sediment to a depth of 80 mm in order to constrain the labeling and the sampling area. The two frames were treated as duplicates (n =2) and were divided in a 100×100 mm sampling grid. Unlabeled control samples were taken just outside the frames as described below. The in-situ labeling experiment started by spraying the surface of the sediment within each frame with 200 ml of [^{13}C] sodium bicarbonate (99% ^{13}C; Cambridge Isotope Laboratories, Andover, USA) with ambient salinity (30‰) to obtain a final concentration of 1 g ^{13}C m^{-2} (Middelburg et al. 2000).

The labeled sediment was sampled 2 and 4 h after label addition during the first low tide (the pulse-labeling period), and subsequently at 12 h, 1 d, 2 d, 3 d, and 5 d exactly at low tide (the chase period). At each sampling time, pore water was collected from two randomly chosen positions within the sampling grid of each stainless-steel frame using porous polymer sippers (Rhizon Soil Moisture Sampler; Eijkelkamp Agrisearch Equipment) inserted into the upper 15 mm of the sediment and these two samples were combined (total ~5 ml). For each stainless-steel frame, 1 ml of pore water was injected into airtight headspace vials and analyzed for ^{13}C-DIC (dissolved inorganic carbon) and the remainder was used for inorganic nutrient analysis and short chain organic acid (SCOA) analysis. Water column nutrient data were obtained from the Netherlands Institute for Sea Research (NIOZ) monitoring program from a station 500 m away from the experimental site.

Sediment samples were collected and mixed from two randomly chosen positions within the sampling grid of each steel frame. The top 15 mm of the sediment was collected by pushing a core liner (inside diameter 100 mm) into the sediment to a depth of 50 mm and subsequently the top 15 mm of the sediment was sampled with a spatula (Middelburg et al. 2000). The corer was removed and the sampling hole was filled with unlabeled sediment collected just outside the experimental area. The two sediment samples taken from each steel frame area were homogenized and subsampled for the various analyses. Samples for phospholipid-derived fatty acids (PLFA) analysis were directly frozen in liquid nitrogen and subsequently lyophilized and stored at -20 ^{o}C until analysis. Samples for pigment analysis were also directly frozen in liquid nitrogen and were subsequently stored at -80 ^{o}C prior to analysis. Sediment samples for EPS extraction were transported to the laboratory within 30 min after sampling and subsequently processed as described in Miyatake et al. (2014). For all experiments, two operationally defined EPS were extracted: water-extractable EPS (EPS MQ) using freshly prepared Milli-Q water (MQ, 18.2 MΩ, DOC free, Millipore, Bedford, MA, USA) and EDTA-extractable EPS (EPS EDTA). To ~4 g wet weight of the homogenized sample 4.5 ml Milli-Q water

was added for EPS MQ extraction as described in de Brouwer & Stal (2001). Samples were shaken for 1 h at 30 ^{o}C in the dark and centrifuged at 4,000 × g for 15 min and the supernatant was stored at -20 ^{o}C. The pellet was re-extracted with 4.5 ml of 0.1 M EDTA by shaking for 4 h in the dark at room temperature. The supernatant was collected after centrifugation at 4,000 × g for 15 min and stored at -20 ^{o}C. Both extracts were analyzed for carbohydrates (CHO) and amino acids (AA). In total four operationally defined EPS fractions were distinguished: CHO MQ, CHO EDTA, AA MQ and AA EDTA.

In order to study dark fixation by chemoautotrophic and heterotrophic bacteria, two cores (70 mm inner diameter) were taken outside the experimental area and incubated in the dark for 4 h with the same amount of ^{13}C-label (per m^{2}) as used in the experimental area added to the top of the sediment. The top 15 mm of the core was sampled and analyzed for PLFA labeling.

Miniaturized pulse amplitude modulated (PAM) fluorimetry (Mini-PAM, Walz GmbH, Effeltrich, Germany) was used to measure photosynthetic parameters. Intact sediment cores of the diatom mat were taken in duplicate. Rapid light curves (RLCs) were recorded simultaneously with the pulse-labeling period. Prior to RLCs recording, samples were dark adapted for 15 min to relax photochemical quenching. Subsequently, RLCs were recorded with 12 incremental irradiance steps of 20 s. From these data, the relative maximum photosynthetic electron transport, the light affinity coefficient (alpha), and the light saturation irradiance were determined (Serôdio et al. 2005).

During the ^{13}C label incorporation and RLCs recordings, PAR (400-700 nm) was measured on site every 15 min by a LICOR light meter (LI-250A) connected to a quantum sensor (LI-190R, Li-cor, Lincoln, NE, USA). Throughout the year, a PAR sensor (Licor, LI 191) connected to a data logger

(Licor, LI-1000), located 10 km from the study area, measured PAR values every minute; these data were averaged and logged hourly. The light sensors were cosine corrected.

Analytical procedures

For DIC analysis, pore water samples were acidified by adding 0.1 ml of 19 M phosphoric acid (Miyajima et al. 1995) and headspace gas was analyzed by elemental analyzer/isotope ratio mass spectrometry (EA/IRMS) in order to determine the concentration and isotopic composition of DIC.

Carbon content and isotopic composition of EPS and SCOA were analyzed by LC/IRMS. For carbohydrates, 4 ml EPS extract was hydrolyzed under acidic conditions to monosaccharides using a modified method according to Cowie & Hedges (1984). The method was modified by neutralizing the hydrolyzed samples with strontium carbonate instead of barium carbonate, which resulted in an increased yield of the extract. For the EPS EDTA extracts the EDTA was removed from the hydrolyzed samples as described in Moerdijk-Poortvliet et al. (2014). Carbohydrates were analyzed by LC/IRMS as described in Boschker et al. (2008). For amino acids, 4 ml EPS extract was hydrolyzed with 6 M HCl for 20 h at 110 ^{o}C and subsequently purified by cation exchange chromatography (Veuger et al. 2005) and analyzed by LC/IRMS as described in McCullagh et al. (2006). SCOA were analyzed without additional sample preparation and analyzed by LC/IRMS equipped with an Aminex HPX-87H cation exchange column (Bio-Rad Laboratories, Hercules, USA). The eluent was 8 mM sulfuric acid at a flow rate of 0.4 ml min^{-1} (Krumböck & Conrad 1991). Liquid chromatography was carried out using a Surveyor liquid chromatograph connected to an LC Isolink interface and a Delta V Advantage IRMS (all from Thermo Fisher Scientific, Bremen, Germany).

Lipids were extracted from 4 g dry weight of sediment with a modified Bligh and Dyer extraction (Boschker et al. 1999). The lipid extract was fractionated on silicic acid (60, Merck) into different

polarity classes by sequential eluting with chloroform, acetone and methanol. The chloroform fraction contained mainly neutral lipid-derived fatty acids, while the acetone and methanol fraction contained polar lipids-derived fatty acids (i.e. mainly glycolipids-derived fatty acids and phospholipid-derived fatty acids (PLFA), respectively, but both fractions also contained other lipids such as betaine lipids and sulfolipids) (Heinzelmann et al. 2014). The methanol fraction was denoted as the PLFA fraction and converted into fatty-acid methyl esters, and the carbon content and isotopic composition of these derivatives were measured by gas chromatography isotope ratio mass spectrometry (Middelburg et al. 2000, Boschker 2004).

Pigments were extracted with acetone (90%, buffered with 5% ammonium acetate) from freeze-dried sediment and analyzed by reverse-phase high-performance liquid chromatography (Dijkman & Kromkamp 2006).

Nutrients were measured using a segmented continuous flow analyzer (SEAL QuAAtro XY-2 autoanalyzer, Bran and Luebbe, Norderstedt, Germany) according to the instructions provided by the manufacturer.

Data analysis

The absolute amount of ^{13}C incorporated into EPS fractions, SCOA and PLFA in excess of the background was displayed. This value is expressed as excess ^{13}C and is calculated from $\delta\ ^{13}C_{sample}$ as:

Excess ^{13}C (mol $^{13}C\ m^{-2}$) =

$$\left[\left(\frac{\left(\delta^{13}C_{sample}/1000+1\right)\times R_{st}}{\left(\delta^{13}C_{sample}/1000+1\right)\times R_{st}+1}\right)-\left(\frac{\left(\delta^{13}C_{background}/1000+1\right)\times R_{st}}{\left(\delta^{13}C_{background}/1000+1\right)\times R_{st}+1}\right)\right]\times C_{sample}$$

where $\delta^{13}C_{background}$ denotes the $\delta^{13}C$ value of the unlabeled sample and C_{sample} denotes the pool size in mol of carbon per square meter sediment (mol C m^{-2}). Production rates of various EPS fractions and PLFA biomarkers were quantified by calculating the regression slope from sample data (at 0, 2, and 4 h) (expressed in μmol ^{13}C m^{-2} h^{-1}).

Excess ^{13}C into bacterial biomass was estimated from the label incorporated in bacterial-biomarker PLFA as excess ^{13}C-bacterial biomass (mol ^{13}C m^{-2}) = Σ excess ^{13}C $PLFA_{bact}$/(0.056 × 0.23), where ^{13}C $PLFA_{bact}$ is ^{13}C in bacterial-biomarker PLFA (i.e. i14:0, i15:0, ai15:0, i17:0, 17:1ω6c, cy-19:0, i17:1ω7c, 10Me16:0, and i17:1ω5c), 0.056 represents the average PLFA content in bacteria in terms of carbon, and 0.23 ± 0.06 is the average fraction of these bacterial PLFA among total PLFA in bacteria-dominated marine sediments (Middelburg et al. 2000). Excess ^{13}C into diatom biomass was calculated from the difference between excess ^{13}C into all PLFA and excess ^{13}C into bacterial PLFA and was also corrected for the typical PLFA content of diatoms: excess ^{13}C-diatom biomass (mol^{13}C m^{-2}) = (Σ excess ^{13}C $PLFA_{all}$-Σ excess^{13}C $PLFA_{bact}$)/0.035, where ^{13}C $PLFA_{all}$ is ^{13}C in all individual PLFA measured and 0.035 represents the average PLFA content of diatoms (Middelburg et al. 2000). Diatom and bacterial biomass were calculated as above in terms of carbon per m^2 sediment using the PLFA concentrations instead of excess ^{13}C values.

The relative photosynthetic electron transport rate (rETR) was calculated by multiplying the Mini PAM measured quantum yield (i.e. 'efficiency' of photosynthesis) and the applied irradiance (E) during the recording of the RLCs (Kromkamp & Forster 2003). From the RLCs the relative maximum photosynthetic electron transport rate (ETR_{max}), the light affinity coefficient in the light limited region of the rapid light curve (alpha), and the light saturating irradiance (E_k= ETR_{max}/alpha) were determined by fitting the RLCs to a modified version of the equation of Eilers & Peeters (1988): $rETR=E/aE^2 + bE + c$), where $a=(alpha \times E_k^2)^{-1} - 2 \times (alpha \times E_k)^{-1}$; $c=alpha^{-1}$.

241

242 Multivariate statistics were applied in order to identify the relationships between environmental,
243 photosynthetic, and pigment parameters (i.e. explanatory variables; Supplementary Table S1) and
244 production rates of the EPS fractions (Supplementary Table S2). The various EPS fractions might
245 have originated from different processes and were correlated to the explanatory variables in such a
246 way that the variables of the EPS fractions were kept in separate tables (samples × variables). The
247 relationships between the explanatory variables and the different EPS fractions were explored by
248 Concordance Analysis (Lafosse & Hanafi 1997). This approach is an extension of Co-Inertia analysis
249 (Dolédec & Chessel 1994) that matches one table to several others. The inherent logics of Co-Inertia
250 enables to proceed with a large number of variables (Dray et al. 2003). Concordance Analysis
251 searches combinations of variables in each EPS fraction that co-vary and vary with combinations of
252 explanatory variables. The number of variables does not affect the strength of the correlation because
253 the tables are weighted by the inverse of their respective inertia. Because the EPS fraction data were
254 percentages they were *log*-transformed and centered in column as recommended for compositional
255 data (Aitchinson 1983). Explanatory variables were *log*-transformed and normalized. Prior to
256 Concordance Analysis, the correlation between the explanatory variables and each EPS fraction was
257 assessed by the *Rv* coefficient (Robert & Escoufier 1976). The significance was tested by a
258 randomization procedure of 9999 permutations of table lines (Heo & Gabriel 1998). Hence, only the
259 significantly correlated part of EPS to explanatory variables was considered in the Concordance
260 Analysis. In the case of a single significantly correlated EPS table, the Concordance Analysis was a
261 simple Co-Inertia analysis. Concordance Analyses were run with ADE-4 software (Thioulouse et al.
262 1997) and associated graphical representations were made with the "ade4" package (Chessel et al.
263 2004) in R version 3.2.3 (R Core Team 2015).
264

RESULTS

Seasonal dynamics of exudation and heterotrophic consumption of EPS and SCOA

An overview of the ^{13}C label in the exuded carbon by benthic diatoms, i.e. EPS and SCOA, is depicted in figure 1. In the two operationally defined EPS extracts (i.e. EPS MQ and EPS EDTA) we measured carbohydrates (CHO) as well as amino acids (AA) and, hence, we assigned four EPS fractions (CHO MQ, CHO EDTA, AA MQ and AA EDTA). The ^{13}C labeling of bacteria (through the analysis of PLFA biomarkers) originated from the heterotrophic consumption of the extracellular carbon compounds released by the diatoms.

Most of the ^{13}C label was recovered in CHO MQ, followed by CHO EDTA, AA MQ, AA EDTA and SCOA. The highest amount of ^{13}C label in all of these pools was observed in February and April (Fig. 1). Especially in February and April an initial steep increase of ^{13}C label was observed in the exuded carbon pools, which was followed by a steep decrease. During the rest of the year (June – December), EPS and SCOA were exuded and consumed at lower rates. The amount of ^{13}C label incorporated into the EPS and SCOA was highest between 4 - 12 h after the application of the label and subsequently disappeared during the course of the experiment (Fig. 1). The data suggest that the initial release of exudates was followed by a second (between 24 - 48 h) and sometimes even by a third release (between 48 - 72 h). Labeling of the bacterial PLFA increased sharply during the first 4 h of the experiment and fluctuated during the course of the experiment. The increase of ^{13}C label in bacterial biomarkers coincided with the release of EPS and SCOA.

Exudation and fate of EPS and SCOA carbohydrates and amino acids

Throughout the year, carbohydrates formed the main component of the extracellular fractions (68-91%) while a small part represented amino acids (9-32%) (Fig. 2a). Carbohydrate also explained most

289 of the production of EPS (80-95%) (Fig. 2b). EPS production was strongly seasonal, while the EPS
290 content of the sediment was less strongly affected by the season.
291
292 Figure 3 depicts the content of carbohydrates and amino acids of the EPS MQ and EPS EDTA
293 extracts 4 h after the application of ^{13}C label (Fig. 3a, b, c, d) and after 3 days (Fig. 3e, f, g, h). This
294 time-was chosen, because from day 3 onwards the ^{13}C label distribution remained more or less the
295 same. For carbohydrate as well as for amino acids, the relative ^{13}C label distribution in the monomers
296 of the extracted EPS was different. For the CHO MQ fraction most of the ^{13}C label was incorporated
297 into glucose (80±11%) (Fig. 3a) while in the CHO EDTA the ^{13}C label was more evenly distributed
298 between the monomeric carbohydrates (Fig. 3b). Most of the ^{13}C label in the AA MQ fraction was
299 incorporated into proline (54±11%) (Fig. 3c) while in the AA EDTA the highest amounts of ^{13}C label
300 were found in threonine, serine and valine and depended on the season (Fig. 3d). Due to the elution of
301 an unknown compound in the chromatogram of the AA EDTA fraction (which was substantial and
302 comprised a large part of the chromatogram), the amino acids glycine, proline and alanine could not
303 be determined. Despite this limitation, it was ascertained that the AA EDTA fraction contained
304 aspartate, serine, threonine and methionine, which were not retrieved in the AA MQ fraction.
305 Similarly, the AA MQ fraction contained phenylalanine, lysine and tyrosine, which were absent in the
306 AA EDTA fraction. Besides the different monomeric composition of the extracted EPS fractions, also
307 the ^{13}C label distribution in the monomers varied seasonally (pie charts Fig 3a, b, c, d).
308
309 Up to 23±4% of the total fixed carbon in the carbohydrate pool was exuded as EPS MQ and up to
310 6±1% as EPS EDTA. Similarly, most of the total fixed carbon in the amino acid pool was exuded as
311 EPS MQ rather than as EPS EDTA (46±25% and 7±2%, respectively). The percentage of carbon that
312 was initially fixed as carbohydrate and amino acid and subsequently exuded as EPS was in general
313 lowest in June (on average 3±2%) (Fig. 3a, b, c, d, dotted line).

314

315 The ^{13}C label incorporated into the EPS during the first 4 h of the experiment disappeared to a large
316 extent during the course of the experiment (Fig. 3e, f, g, h). This was particularly the case for CHO
317 MQ in which only 20±9% of the ^{13}C label remained after 3 days (Fig. 3e). For CHO EDTA and AA
318 MQ the decrease of ^{13}C label after 3 days was less (59±21% and 75±32% of the incorporated ^{13}C label
319 remained, respectively). In the case of AA EDTA, 39.3 ±19.2% remained after 3 days, except in
320 December when a substantial net label increase was found (Fig. 3h). An increase in the proportioning
321 of deoxy-sugars (fucose and rhamnose) was found in EPS MQ and EPS EDTA while glucose
322 decreased (Fig. 3e, f). Similarly, a shift in the distribution of amino acids was observed.

323

324 The loss of ^{13}C label from the different EPS fractions showed differences among seasons. In case of
325 the CHO MQ and AA MQ fractions more label remained 3 days after the application of the label in
326 April and June when compared to other months (Fig. 3e, g, dotted line). In case of the CHO EDTA
327 fraction less ^{13}C label remained 3 days after the start of the experiment in February and April, whereas
328 less ^{13}C label remained in the AA EDTA fraction in February and August when compared to other
329 months.

330

331 The SCOA in the pore water was composed of formate, acetate, oxalate, malate, lactate and succinate.
332 Lactate and succinate could not be separated sufficiently well using our LC protocol and are therefore
333 reported as the sum of both. Considerable seasonal changes in the ^{13}C labeling of succinate/lactate,
334 formate and acetate were observed. Other SCOA were below the limit of detection; hence, only
335 succinate+lactate, formate and acetate are depicted in figure 4. The concentrations of
336 succinate+lactate (range 2.7-5.7 μM), formate (range 3.7-13.6 μM), and acetate (range 1.0-5.8 μM) in
337 the pore-water were high. Labeling of succinate/lactate, formate and acetate were highest in February
338 and gradually decreased during the year. The percentage of ^{13}C label that remained in all SCOA 3

339 days after the start of the experiment increased during the year and ranged from 5% in February to
340 42% in December.
341
342 **Explanatory variables**
343 Nutrient concentrations in the pore water were always higher than in the water column above the
344 sediment (during immersion) (Supplementary Table S1). Inorganic nitrogen was predominantly
345 present as ammonium in the pore water and as nitrate in the overlying water. Average concentrations
346 of pore water inorganic nitrogen were lower in summer (June and August) compared to the rest of the
347 year (respectively 27.9±0.1 and 72±27 μmol l^{-1}). N:P ratios above the Redfield ratio (i.e. 16) were
348 observed from February until June (26±5). In August and October N:P ratios were below the Redfield
349 ratio (7±1) and in December near the Redfield ratio (17±1) (Supplementary Table S1). Likewise, the
350 concentration of inorganic nitrogen in the overlying water was lower in summer (June and August)
351 compared to the rest of the year (respectively 14±3 and 38±16 μmol l^{-1}). The seasonal trend of
352 nutrient N:P ratios in the overlying water was similar as in the pore water and were above the Redfield
353 ratio from February until June and in December (46±30) and below the Redfield ratio in August and
354 October (12±2) (Supplementary Table S1). The pigment fingerprints were typical for diatoms,
355 including β-carotene, chlorophyll *a*, chlorophyll *c*, fucoxanthin, diadinoxanthin and diatoxanthin
356 (Supplementary Table S1). The photosynthetic parameters E_k and ETR_{max} were higher in spring and
357 summer, while α was higher in autumn and winter (Supplementary Table S1). PAR correlated to the
358 sediment temperature and was higher in summer than in winter. The average temperature and
359 integrated photon irradiance during the 4 h of ^{13}C labeling of the diatom mat were lowest in February
360 (3.7 ^{o}C and 1,314 μmol photons m^{-2} and highest in August (20.5 ^{o}C and 7,492 μmol photons m^{-2})
361 (Supplementary Table S1).
362
363 **Production and fate of EPS in relation to explanatory variables**

Concordance Analysis was done using the dataset of the incorporation rate of ^{13}C label in monomeric carbohydrates and monomeric amino acids in the EPS extracts (i.e. CHO MQ, CHO EDTA, AA MQ and AA EDTA) (Supplementary Table S2) and explanatory variables (Supplementary Table S1). The *Rv* coefficients between the explanatory variables and three EPS fractions were significant (p-value < 0.05); CHO MQ was not significant) (Table 1). Results from the Concordance Analysis are depicted in figure 5. The first two axes express the major dynamics among the four seasonal clusters (i.e. February, April, June/August and October/December).

The first axis of the Concordance Analysis of the three EPS fractions (i.e. CHO EDTA, AA MQ, and AA EDTA) opposed autumn and winter (i.e. October, December and February) from spring and summer (i.e. April, June and August), whereas the second axis opposed months during which a high EPS production took place (i.e. February and April) to months with a low EPS production (i.e. June, August, October and December) (Fig. 5). The nature of the predominant monomeric carbohydrates and amino acids characterized the seasonal clusters (Fig. 5d, e, f).

Along the first axis of the Concordance Analysis, the carbohydrates of the EPS (i.e. CHO EDTA fraction) (Fig. 5a) exuded during spring and summer (April, June, and August) showed higher production rates of xylose and rhamnose, and a lower production rate of galactose. In contrast, in autumn and winter (October, December, and February) a high production rate of galactose was observed. Along the second axis, months with a high EPS production (i.e. February and April) show higher fucose production. The months with a low EPS production (i.e. June, August, October, and December) show a high mannose production.

Similar as was the case for the carbohydrate component of the EPS, along the first axis of the Concordance Analysis the AA MQ fraction (Fig. 5b) showed a higher production rate in spring and

summer for all amino acids except glycine and proline, which had a lower production rate. Along the first axis, autumn and winter showed a high production rate of glycine and proline and a low production rate of the other measured amino acids. Along the second axis a high production rate of tyrosine and a low production rate of valine were observed. Different than what was seen for the CHO EDTA and AA MQ fractions, the AA EDTA fraction showed a high production rate for most amino acids during June, August, October, and December (i.e. when the production of EPS was low) except for threonine (Fig. 5c). Threonine production rates were high in February and April (i.e. when EPS production was high).

The first axis of the Concordance Analysis was strongly characterised by temperature and positively associated to PAR, ETR_{max}, and E_k (Fig. 5g). Temperature and PAR decreased from June/August to October/December and were associated with an increase in alpha (i.e. the affinity of photosynthesis for light), β-carotene content, and phosphate- and ammonium concentration in the overlying water. Along the first axis, the increased rates of synthesis of the majority of carbohydrate monomers and amino acids of the CHO EDTA and AA MQ fractions were mainly covariant with light intensity and, to a lesser extent, with sediment temperature, E_k and ETR_{max} (Fig. 5a, b, g). Along the second axis, increased rates of synthesis of amino acids of the AA EDTA fraction were observed. These increased rates of synthesis were consistently associated with a low content of light-harvesting pigments and possibly with insufficient ammonium in the pore-water or nitrate in the water column (Fig. 5c, g). Moreover, the high rates of EPS production in February and April were consistently associated with a high content of light harvesting pigments and high concentrations of ammonium in the pore-water or nitrate in the water column (Fig. 5g).

At day 3 after the start of the experiments, the relationship between the proportioning of ^{13}C label in the CHO MQ, AA MQ, and AA EDTA fractions (Supplementary Table S3) and explanatory variables

414 (Supplementary Table S1) were significant (Table 1). The pattern resulting from the Concordance
415 Analysis was expressed along two main axes (Fig. 6g). There was no relationship between the ^{13}C
416 label proportioning of the CHO EDTA fraction at day 3 and the explanatory variables (*p*-value >
417 0.05). A seasonal succession similar to the one from the distribution pattern at t = 4h was observed,
418 although the pattern rotated by opposing spring and summer (i.e. April, June and August) to autumn
419 and winter (i.e. October, December and February) on the second axis (Fig. 6d, e, f). This opposition is
420 seen in the CHO MQ fraction by increases in rhamnose and mannose from autumn and winter to
421 spring and summer, and increases in xylose and fucose from summer and autumn (i.e. June, August
422 and October) to winter and spring (i.e. December, February and April) (Fig. 6a, d). For the AA MQ
423 and AA EDTA fractions, the interplay among variables from the ^{13}C label distribution pattern at day 3
424 (Fig. 6b, c) was similar to the one for the distribution pattern at t = 4h (Fig. 5b, c), except for serine
425 and tyrosine in the AA MQ fraction and leucine, isoleucine and valine in the AA EDTA fraction (Fig.
426 6c). At t = 4h, serine and tyrosine in the AA MQ fraction, and leucine, methionine, isoleucine and
427 valine in the AA EDTA fraction were positioned in respectively the June/August and
428 October/December cluster of the concordance plot (Fig. 5b, c). At day 3, serine and tyrosine did not
429 occur in the AA MQ fraction (Fig. 6b) and leucine, isoleucine and valine in the AA EDTA fraction
430 were positioned in the February and April clusters (Fig. 6c). This implies that serine and tyrosine (AA
431 MQ fraction), and leucine, isoleucine and valine (AA EDTA fraction) ^{13}C label dynamics were
432 different than for the other amino acids and ^{13}C label loss of these amino acids in February and April
433 was low.
434
435 **Seasonal development of the diatom mat**
436 Benthic diatoms were visible at the sediment surface during the whole year but varied in density,
437 depending on the time of the year and the time of the day. Both the biomass of benthic diatoms and
438 benthic bacteria as estimated from fatty acids biomarker data were lower during summer (June and

August) (Fig. 7a). The decrease in biomass coincided with the activity of bioturbating fauna that grazed and disturbed the diatom mat. The annual ratio of diatom to bacterial biomass was constant at ~4.6 (Fig. 7a). The production rate of diatoms and bacteria decreased during the year and was lowest in October and December (Fig. 7b). During February, April, and June the biomass of diatoms and bacteria seemed to be coupled, as seemed to be the case for the productivity of both groups of organisms. From August onwards, the coupling of the growth of diatoms and bacteria deteriorated and had almost disappeared in December (Fig. 7b). This pattern was retained until day 3 of the experiment (Fig. 7c). On average, only 1.7±0.9% of the initially applied ^{13}C-DIC remained 12 h after the start of the experiment, confirming that most of it was washed out (or exchanged with the atmosphere). In addition, dark fixation of ^{13}C label, as was determined in separate sediment core experiments, indicated that CO_2 fixation by chemoautotrophic bacteria or through anaplerotic carbon fixation by heterotrophs was not detected in PLFA in dark incubated (4 h) cores (see Material and Methods) (results not shown), which is in agreement with the conclusions drawn by Miyatake et al. (2014). Hence, the ^{13}C label incorporation in heterotrophic bacteria in this study was mainly due to the transfer of organic matter between diatoms and bacteria.

The production and fate of PLFA bacterial biomarkers

The ^{13}C label incorporation in bacterial biomarkers was high at the beginning of the year and gradually decreased towards the end of the year (Fig. 8a). In the first half of the year (i.e. February, April, and June) ^{13}C incorporation was dominated by the iC17:ω7c, 10MeC16:0 and iC17:1ω5c biomarkers, whereas in the second half of the year (i.e. August, October, and December) other PLFA biomarkers took over (Fig. 8a, pie charts).

During the year the ^{13}C incorporated in the bacterial biomarkers iC17:ω7c, 10MeC16:0 and iC17:1ω5c decreased after 3 days (Fig. 8). This was in contrast to other PLFA, which increased their

label content (Fig. 8). During February, April, and June on average 77±15% of the initially incorporated ^{13}C label remained after 3 days (Fig. 8b, dotted line). This was in contrast to the months August, October, and December when a net gain of label ^{13}C was observed. On average 459±207% of label was gained compared to the amount of incorporated ^{13}C label at t = 4h (Fig. 8b, dotted line).

DISCUSSION

Production and fate of carbohydrates and amino acids of diatom EPS

The composition of the EPS produced by benthic diatoms is complex and degradation of this material by microorganisms is a largely unexplored process. The exuded EPS consisted mainly of carbohydrate but amino acids are a component that is consistently present. This type of EPS is common for diatom dominated biofilms (Granum et al. 2002). Bacterial biofilm assemblages are dominated by proteins rather than by polymeric carbohydrates (Flemming et al. 2000). The composition of the extracted fractions of EPS (EPS MQ and EPS EDTA) differed with respect to the carbohydrates and amino acids. This suggests that the synthesis of these two operational defined EPS extracts is under different metabolic control. The carbohydrate composition of EPS MQ was rich in glucose and it was produced at a higher rate than the other fractions, suggesting a direct relationship with photosynthesis (de Brouwer & Stal 2001). Glucose can be directly incorporated from chrysolaminaran, while other carbohydrates need to be synthesized first from glucose and therefore this would take longer to produce (Underwood & Paterson 2003). Exudates with high glucose content are usually a source of easy degradable carbon for microorganisms. In contrast to EPS MQ, EPS EDTA was rich in deoxysugars (e.g. fucose and rhamnose) and pentoses (e.g. xylose). Deoxysugars and pentoses contribute to the adhesive properties of EPS (Underwood & Paterson 2003) and are more refractory towards degradation (Giroldo et al. 2003).

Although amino acids are a minor component of the EPS in benthic diatom mats, they are important for the structure and properties of these polymers. Lectins (i.e. carbohydrate-binding proteins) link the polysaccharide chains in EPS and are thereby contributing to the tertiary structure. This is essential for the biofilm structure, adhesion, and stability (Dugdale et al. 2006). For example, it has been suggested that EPS-proline and EPS-glycine cause adhesion between organisms in soils and give elasticity to the EPS matrix (Redmile-Gordon et al. 2015). The amino acid proline is known to be multifunctional and its enhanced synthesis could be an important factor in stress acclimation (e.g. salt- and oxidative stress) and serves as osmo-protectant in certain microorganisms (Van Bergeijk et al. 2003, Szabados & Savoure 2010). Extracellular proline may also serve as an anti-freeze allowing the presence of liquid water at low temperatures (Wiencke 2011). We conceive that similar functions can be attributed to proline and glycine in diatom mats, particularly because the synthesis of proline and glycine is enhanced in autumn and winter. EPS with a high content of proline and glycine could serve as anti-freeze and increases elasticity of the EPS matrix of the diatom mat. In this study, we also observed that threonine (in the AA EDTA fraction) was a distinctive and characteristic amino acid because of its high synthesis rate in February and April; i.e. when EPS was produced at high rates. Threonine is known to be associated with algal defense (Buhmann et al. 2016) and therefore might play a role in controlling bacterial activity during the period of high EPS productivity in February and April. In addition, extracellular amino acids are part of enzymes, nutritious polymers or serve as signaling molecules that play a role in diatom cell adhesion and defense processes (Buhmann et al. 2016). Knowledge about the functionality of the substances exuded by diatoms is still limited, but we conceive that the exudation of carbohydrates serves two main purposes, namely to allow diatom motility and to maintain their redox balance. At the ecosystem level these exudations represent an important carbon- and energy source, although due to a lack of nitrogen and other nutrients they are also considered poor food sources for higher trophic levels.

513 EPS production often changes with the growth phase of the organism, with the level of irradiance or
514 availability of nutrients, or may be linked to endogenous cell rhythms (Underwood & Paterson 2003).
515 The carbon fixed by the benthic diatoms in the present study was exuded rapidly (within 2 h), which
516 agrees with the idea of EPS exudation during photosynthesis as has been suggested by Underwood &
517 Paterson (2003). We observed that a substantial proportion (between 9 and 21%) of the fixed carbon
518 was exuded in the environment as EPS. Other authors reported that this range of fixed carbon released
519 as exudates may be even larger: i.e. between 1.7 to 73%, with a median value between 30-40%
520 (Underwood & Paterson 2003).
521
522 EPS exudation followed a seasonal pattern with a lower percentage of fixed carbon exuded in summer
523 compared to the rest of the year and showed a significant relation with explanatory variables such as
524 light intensity, temperature and nutrient concentrations. We conceive that the type of EPS differs
525 depending on the season and that this is related to different functions of EPS; overflow metabolism or
526 motility. A dense diatom mat rapidly depletes the nutrients from the small volume of pore-water. A
527 lack of nutrients during photosynthesis makes a balanced synthesis of structural cell material
528 impossible. This will result in a situation of unbalanced growth during which the product of
529 photosynthesis is diverted to carbohydrate (overflow metabolism). Eventually, when the intracellular
530 pool of the storage carbohydrate chrysolaminaran is filled up, the excess carbohydrate is exuded as
531 EPS (Stal 2010). Especially in February and April (i.e. high productivity months and a dense diatom
532 mat), the production of EPS should be intimately related with the rate of photosynthesis (de Brouwer
533 and Stal 2001) and EPS exudation served as an overflow valve for excess energy (Stal 2010). In June
534 and August, the diatom mat was less dense and EPS production might be the result of motility because
535 the diatoms are forced to migrate because of sediment burial due to bioturbation and/or in order to
536 escape high light intensities (Consalvey et al. 2004). During the summer, the diatoms are exposed to a
537 higher faunal grazing pressure (Pinckney et al. 2003). In October and December bioturbation and

538 grazing are much less and overflow metabolism takes over again. In addition, EPS produced in
539 summer was more heterogeneous probably because the higher synthesis rates of most of the
540 carbohydrate monomers and amino acids. Hence, EPS produced in summer was different in structure
541 compared to the other seasons and their physicochemical properties may therefore be different. These
542 different physicochemical properties could have affected their function and fate in the sediment such
543 as their hydrophobicity and degradability by heterotrophic bacteria (Giroldo et al. 2003). For example,
544 an increase in heterogeneity of EPS in terms of the carbohydrate monomers and amino acids could
545 lead to a more complex structure and a higher recalcitrance to microbial degradation.
546
547 The ^{13}C label dynamics of CHO MQ indicated a high turnover. The high loss of CHO MQ can be
548 partially explained by the washout during tidal inundation, which may account for up to 60% of the
549 EPS loss from the sediment (Underwood & Smith 1998, Hanlon et al. 2006). However, heterotrophic
550 bacteria also consume EPS. This was demonstrated by the enrichment of ^{13}C of bacterial specific
551 PLFA biomarkers coinciding the loss of CHO MQ and this agrees with other studies. (Goto et al.
552 2001, Miyatake et al. 2014). EPS EDTA was less influenced by tidal washout and was more refractory
553 against bacterial consumption, which explained its slower turnover. This is consistent with previous
554 studies reporting that deoxy-sugar rich EPS are tightly bound to the sediment and are recalcitrant to
555 bacterial degradation, while hexose-rich polymers are colloidal and more rapidly degraded (de
556 Brouwer and Stal 2001, Giroldo et al. 2003, Hanlon et al. 2006). However, despite these losses,
557 continued isotopic enrichment of EPS indicated new production at the expense of another enriched
558 compound. This enriched compound may be an intracellular carbon source such as chrysolaminaran
559 or an extracellular carbon source such as material derived from degradation of more refractory EPS.
560 Chiovitti et al. (2003) suggested the appearance of a pathway by which EPS EDTA becomes available
561 in the EPS MQ pool by bacterial degradation. For instance, by selective consumption of glucose-rich
562 parts of EPS MQ leaving the more refractory EPS EDTA. Stal (2010) suggested that EPS EDTA

might have been derived from initially exuded EPS MQ. This hypothesis is supported by the results of the present study. We observed an increase in the deoxy-sugars of EPS as well as an increase in the isotopic enrichment of EPS EDTA between 12 h and 120 h. The transition from one EPS fraction to the other is probably also depending on the concentration of divalent cations present in the sediment, such as Ca^{2+} and Mg^{2+}, which interact with the EPS (Stal 2010). The binding capacity of these cations enables part of EPS MQ to be eventually transformed into EPS EDTA. In this study, we found seasonal differences of the production and fate of carbohydrate monomers and amino acids in EPS.

EPS and SCOA as carbon source for bacteria

Heterotrophic bacteria are omnipresent in diatom mats and utilize organic carbon produced by diatoms (Middelburg et al. 2000, Bellinger et al. 2009). Especially early in the year (February, April and June), the bacterial PLFA biomarkers showed an initial fast uptake of ^{13}C label, which was probably the result of the utilization of low-molecular-weight EPS and SCOA exuded by diatoms. Various groups of bacteria used the diatom exudates as was evidenced by the differences in the level of ^{13}C excess values between PLFA biomarkers. The PLFA i17:1ω7c, i17:1ω5c and 10Me16:0 are known to be specific for sulfate-reducing bacteria (SRB) (Boschker et al. 1998, Boschker & Middelburg 2002). From February until June the biomass and production of diatoms and bacteria seemed to be coupled. It was concluded that during these months SCOA were the most important substrates for the bacteria. Especially SRB benefited from associating with SCOA-releasing diatoms. From August on, the coupling of biomass and production of diatoms and bacteria became less strong and was almost lost in December. During the period of August until December, EPS produced by diatoms promoted the growth of other bacteria than SRB. The production of SCOA was low from August to December. SRB-utilizing SCOA dominated the community during the first half of the year (i.e. February, April, and June) and showed a higher turnover rate than other bacteria, which dominated the community the second half of the year (i.e. August, October, and December). The

588 seasonal variation of exudates produced by the diatoms played an important role in shaping the
589 community composition and diversity of the associated bacteria.
590
591 CHO MQ appeared to be a more important intermediate in the initial transfer of carbon between
592 diatoms and bacteria than CHO EDTA. The amino acids of the EPS were more important in the
593 longer term. After the initial fast transfer of carbon from diatoms to heterotrophic bacteria, a second
594 peak of ^{13}C label incorporation in bacteria coincided with, on the one hand, the disappearance of ^{13}C
595 label in EPS MQ and, on the other hand, the second release of ^{13}C label in EPS MQ and EPS EDTA.
596 It was therefore concluded that this second peak of labeling was due to the ongoing consumption of
597 EPS MQ, as well as due to the consumption of more recalcitrant EPS (after enzymatic hydrolysis to
598 low-molecular-weight compounds) in the long term (Hunter et al. 2006). Degrading complex EPS is
599 slow and the entire process might take as long as a month (Giroldo et al. 2003). CHO EDTA seems to
600 be a less favorable carbon source for heterotrophic bacteria (Giroldo et al. 2003).
601
602 *Acknowledgments.* We thank Erwin Moerdijk, Wanda Moerdijk, Jelle Moerdijk, Jurian Brasser and
603 Gerjan de Ruiter for assisting in the field sample collection and processing of samples in the
604 laboratory.
605
606 LITERATURE CITED
607 Admiraal W, Peletier H, Brouwer T (1984) The seasonal succession patterns of diatom species on an
608 intertidal mudflat: an experimental analysis. Oikos 42: 30-40
609 Aitchison J (1983) Principal component analysis of compositional data. Biometrika 70: 57-65
610 Amin SA, Parker MS, Armbrust EV (2012) Interactions between diatom and bacteria. Microbiol Mol
611 Biol Rev 76: 667-684

612 Bellinger BJ, Underwood GJC, Ziegler SE, Gretz MR (2009) Significance of diatom-derived
613 polymers in carbon flow dynamics within estuarine biofilms determined through isotopic
614 enrichment. Aq Microb Ecol 55: 169-187
615 Boschker HTS (2004) Linking microbial community structure and functioning: stable isotope (^{13}C)
616 labeling in combination with PLFA analysis. In: Kowalchuk GA, de Bruijn FJ, Head IM,
617 Akkermans ADL, van Elsas JD [eds] Molecular microbial ecology volume 2. Kluwer Academic
618 Publishers, Dordrecht, the Netherlands, p 1673-1688
619 Boschker HTS., de Brouwer JFC, T. E. Cappenberg TE (1999) The contribution of macrophyte-
620 derived organic matter to microbial biomass in salt-marsh sediments: Stable carbon isotope
621 analysis of microbial biomarkers. Limnol Oceanogr 44: 309-319
622 Boschker HTS., Middelburg JJ (2002) Stable isotopes and biomarkers in microbial ecology. FEMS
623 Microbiol Ecol 40: 85-95
624 Boschker HTS, Moerdijk-Poortvliet TCW, van Breugel, Houtekamer M, Middelburg JJ (2008) A
625 versatile method for stable carbon isotope analysis of carbohydrates by high-performance liquid
626 chromatography/isotope ratio mass spectrometry. Rapid Comm Mass Spectro 22: 3902-3908
627 Boschker HTS, Nold SC, Wellsbury P, Bos D and others (1998) Direct linking of microbial
628 populations to specific biogeochemical processes by ^{13}C-labelling of biomarkers. Nature 392:
629 801-805
630 Bruckner CG, Rehm C, Grossart HP, Kroth PG (2011) Growth and release of extracellular organic
631 compounds by benthic diatoms depend on interactions with bacteria. Environ Microbiol 13: 1052-
632 1063
633 Buhmann MT, Schulze B, Förderer A, Schleheck D, Kroth PG (2016) Bacteria may induce the
634 secretion of mucin-like proteins by the diatom *Phaeodactylum tricornutum*. J Phycol 52: 463-474
635 Chessel D, Dufour A, Thioulouse J (2004) The ade4 package. I. One-table methods. R News 4: 5–10

636 Chiovitti A, Bacic A, Burke J, Wetherbee R (2003) Heterogeneous xylose-rich glycans are associated
637 with extracellular glycoproteins from the biofouling diatom *Craspedostauros australis*
638 (Bacillariophyceae). Eur J Phycol 38: 351-360
639 Consalvey M, Paterson DM, Underwood GJC (2004) The ups and downs of life in a benthic biofilm:
640 migration of benthic diatoms. Diatom Res 19: 181-202
641 Cowie GL, Hedges JI (1984) Determination of neutral sugars in plankton, sediments, and wood by
642 capillary gas chromatography of equilibrated isomeric mixtures. Anal Chem 56: 497-504
643 De Brouwer JFC, Stal LJ (2001) Short-term dynamics in microphytobenthos distribution and
644 associated extracellular carbohydrates in surface sediments of an intertidal mudflat. Mar Ecol
645 Progr Ser 218: 33-44
646 Dijkman NA, Kromkamp JC (2006) Phospholipid-derived fatty acids as chemotaxonomic markers for
647 phytoplankton: application for inferring phytoplankton composition. Mar Ecol Progr Ser 324:
648 113-125
649 Dolédec S, Chessel D (1994) Co-inertia analysis: an alternative method for studying species-
650 environment relationships. Freshwater Biol 31: 277-294
651 Dray S, Chessel D, Thioulouse J (2003) Co-inertia analysis and the linking of ecological data tables.
652 Ecology 84: 3078-3089
653 Dugdale TM, Willis A, Wetherbee R (2006) Adhesive modular proteins occur in the extracellular
654 mucilage of the motile, pennate diatom *Phaeodactylum tricornutum*. Biophysic J 90: 58-60
655 Edgar LA, Pickett-Heaps JD (1984) Diatom locomotion. Progr Phycol Res 3: 47-88
656 Eilers P, Peeters J (1988) A model for the relationship between light intensity and the rate of
657 photosynthesis in phytoplankton. Ecol Model 42: 199-215
658 Evrard V, Cook PLM, Veuger B, Huettel M, Middelburg JJ (2008) Tracing carbon and nitrogen
659 incorporation and pathways in the microbial community of a photic subtidal sand. Aq Microb
660 Ecol 53: 257-269

661 Flemming HC, Wingender J, Mayer C, Körstgens V, Borchard W (2000) Cohesiveness in biofilm
662 matrix polymers. In: Allison DG, Gilbert P, Lappin-Scott HM, Wilson M [eds] Community
663 structure and cooperation in biofilms, Cambridge University Press, Cambridge, p 87-106
664 Flemming HC, Wingender J (2010) The biofilm matrix. Nature Rev Microbiol 8: 623-633
665 Giroldo D, Vieira AAH, Paulsen BS (2003) Relative increase of deoxy sugars during microbial
666 degradation of an extracellular polysaccharide released by a tropical freshwater *Thalassiosira* sp.
667 (Bacillariophyceae). J Phycol 39: 1109-1115
668 Goto N, Mitamura O, Terai H (2001) Biodegradation of photosynthetically produced extracellular
669 organic carbon from intertidal benthic algae. J Exp Mar Biol Ecol 257: 73-86
670 Granum E, Kirkvold S, Myklestad SM (2002) Cellular and extracellular production of carbohydrates
671 and amino acids by the marine diatom *Skeletonema costatum*: diel variations and effects of N
672 depletion. Mar Ecol Progr Ser 242: 83-94
673 Hanlon ARM, Bellinger B, Hayes K, Xiao G and others (2006) Dynamics of extracellular polymeric
674 substance (EPS) production and loss in an estuarine, diatom-dominated, microalgal biofilm over a
675 tidal emersion-immersion period. Limnol Oceanogr 51: 79-93
676 Heinzelmann SM, Bale NJ, Hopmans EC, Sinninghe Damsté JS, Schouten S, van der Meer MT
677 (2014) Critical assessment of glyco-and phospholipid separation by using silica chromatography.
678 Appl Environ Microbiol 80: 360-365
679 Heo M, Gabriel KR (1998) A permutation test of association between configurations by means of the
680 rv coefficient. Comm Stat Simul Comput 27: 843-856
681 Hoagland KD, Rosowski JR, Gretz MR, Roemer SC (1993) Diatom extracellular polymeric
682 substances: function, fine structure, chemistry, and physiology. J Phycol 29: 537-566
683 Hunter EM, Mills HJ, Kostka JE (2006) Microbial community diversity associated with carbon and
684 nitrogen cycling in permeable shelf sediments. Appl Environ Microbiol 72: 5689-5701

685 Kromkamp JC, Forster RM (2003) The use of variable fluorescence measurements in aquatic
686 ecosystems: differences between multiple and single turnover measuring protocols and suggested
687 terminology. Eur J Phycol 38: 103-112
688 Krumböck M, Conrad R (1991) Metabolism of position-labelled glucose in anoxic methanogenic
689 paddy soil and lake sediment. FEMS Microbiol Ecol 8: 247-256
690 Lafosse R, Hanafi M (1997) Concordance d'un tableau avec K tableaux: définition de K+ 1 uples
691 synthétiques. Rev Statist Appl 45: 111-126
692 MacIntyre HL, Cullen JJ (1996) Primary production by suspended and benthic microalgae in a turbid
693 estuary: Time-scales of variability in San Antonio Bay, Texas. Mar Ecol Progr Ser 145: 245-268
694 McCullagh JSO, Juchelka D, Hedges REM (2006) Analysis of amino acid ^{13}C abundance from human
695 and faunal bone collagen using liquid chromatography/isotope ratio mass spectrometry. Rapid
696 Comm Mass Spectro 20: 2761-2768
697 McKew BA, Dumbrell AJ, Taylor JD, McGenity TJ, Underwood GJC (2013) Differences between
698 aerobic and anaerobic degradation of microphytobenthic biofilm-derived organic matter within
699 intertidal sediments. FEMS Microbiol Ecol 84: 495-509
700 Middelburg JJ, Barranguet C, Boschker HTS, Herman PMJ, Moens T, Heip CHR (2000) The fate of
701 intertidal microphytobenthos carbon: An in situ ^{13}C-labeling study. Limnol Oceanogr 45: 1224-
702 1234
703 Miyajima T, Yamada Y, Hanba YT, Yoshii K, Koitabashi T, Wada E (1995) Determining the stable
704 isotope ratio of total dissolved inorganic carbon in lakewater by GC/C/IRMS. Limnol Oceanogr
705 40: 994-1000
706 Miyatake T, Moerdijk-Poortvliet TCW, Stal LJ, Boschker HTS (2014) Tracing carbon flow from
707 microphytobenthos to major bacterial groups in an intertidal marine sediment by using an in situ
708 ^{13}C pulse-chase method. Limnol Oceanogr 59**:** 1275-1287

709 Moerdijk-Poortvliet TCW, Van Breugel P, Sabbe K, Beauchard O, Stal LJ, Boschker HTS (2017)
710 Seasonal changes in the biochemical fate of carbon fixed by benthic diatoms in intertidal
711 sediments. Limnol Oceanogr on line doi: 10.1002/lno.10648
712 Moerdijk-Poortvliet TCW, Stal LJ, Boschker HTS (2014) LC/IRMS analysis: A powerful technique
713 to trace carbon flow in microphytobenthic communities in intertidal sediments. J Sea Res 92: 19-
714 25
715 Oakes JM, Eyre BD, Middelburg JJ, Boschker HTS (2010) Composition, production, and loss of
716 carbohydrates in subtropical shallow subtidal sandy sediments: Rapid processing and long-term
717 retention revealed by ^{13}C-labeling. Limnol Oceanogr 55: 2126-2138
718 Pierre G, Zhao J-M, Orvain F, Dupuy C, Klein GL, Graber M, Maugard T (2014) Seasonal dynamics
719 of extracellular polymeric substances (EPS) in surface sediments of a diatom-dominated intertidal
720 mudflat (Marennes–Oléron, France). J Sea Res 92: 26-35
721 Pinckney JL, Carman KR, Lumsden SE, Hymel SN (2003) Microalgal-meiofaunal trophic
722 relationships in muddy intertidal estuarine sediments. Aq Microb Ecol 31: 99-108
723 R Core Team (2015) R: A language and environment for statistical computing. R Foundation for
724 Statistical Computing, Vienna, Austria. URL: https://www.R-project.org/
725 Redmile-Gordon MA, Evershed RP, Hirsch PR, White RP, Goulding KWT (2015) Soil organic matter
726 and the extracellular microbial matrix show contrasting responses to C and N availability. Soil
727 Biol Biochem 88: 257-267
728 Robert P, Escoufier Y (1976) A unifying tool for linear multivariate statistical methods: the rv-
729 coefficient. Appl Statist 25: 257-265
730 Serôdio J, Vieira S, Cruz S, Barroso F (2005) Short-term variability in the photosynthetic activity of
731 microphytobenthos as detected by measuring rapid light curves using variable fluorescence. Mar
732 Biol 146: 903-914

733 Smith DJ, Underwood GJC (1998) Exopolymer production by intertidal epipelic diatoms. Limnol
734 Oceanogr 43: 1578-1591
735 Stal LJ (2010) Microphytobenthos as a biogeomorphological force in intertidal sediment stabilization.
736 Ecol Eng 36: 236-245
737 Szabados L, Savoure A (2010) Proline: a multifunctional amino acid. Trends Plant Sci 15: 89-97
738 Taylor JD, McKew BA, Kuhl A, McGenity TJ, Underwood GJC (2013) Microphytobenthic
739 extracellular polymeric substances (EPS) in intertidal sediments fuel both generalist and specialist
740 EPS-degrading bacteria. Limnol Oceanogr 58: 1463-1480
741 Thioulouse J, Chessel D, Dole S, Olivier JM (1997) ADE-4: a multivariate analysis and graphical
742 display software. Statist Comput 7: 75-83
743 Underwood GJC, Kromkamp J (1999) Primary production by phytoplankton and microphytobenthos
744 in estuaries. Adv Ecol Res 29: 93-153
745 Underwood GJC, Smith DJ (1998) Predicting epipelic diatom exopolymer concentrations in intertidal
746 sediments from sediment chlorophyll *a*. Microbiol Ecol 35: 116-125
747 Underwood GJC., Paterson DM (2003) The importance of extracellular carbohydrate production by
748 marine epipelic diatoms. Adv Bot Res 40: 183-240
749 Van Bergeijk SA, Van der Zee C, Stal LJ (2003) Uptake and excretion of
750 dimethylsulphoniopropionate is driven by salinity changes in the marine benthic diatom
751 *Cylindrotheca closterium*. Eur J Phycol 38: 341-349
752 Veuger B, Middelburg JJ, Boschker HTS, Houtekamer M (2005) Analysis of ^{15}N incorporation into
753 D-alanine: A new method for tracing nitrogen uptake by bacteria. Limnol Oceanogr Meth 3: 230-
754 240
755 Wiencke C (2011) Biology of polar benthic algae. Walter de Gruyter, Berlin, pp 329

Yallop ML, De Winder B, Paterson DM, Stal LJ (1994) Comparative structure, primairy production and biogenic stabilization of cohesive and noncohesive marine-sediments inhabited by microphytobenthos. Est Coast Shelf Sci 39: 565-582

Conflict of Interest

None declared

763 **Table 1.**

764 Correlations in the Concordance Analyses. *Rv* coefficients range from 0-1 and indicate the correlation
765 between the explanatory table and each EPS table. Correlations between axis scores indicate the
766 congruence per axis between the black dots (explanatory) and arrow tips (EPS fraction) in figure 5
767 and figure 6. Bold values indicate significance at the rejection level $\alpha = 0.05$.

768

EPS fraction	**Explanatory *vs* Production EPS**			**Explanatory *vs* ^{13}C label day-3 EPS**		
	Rv	Pearson's *r* 1st axis	Pearson's *r* 2nd axis	*Rv*	Pearson's *r* 1st axis	Pearson's *r* 2nd axis
CHO MQ	0.37	_	_	**0.43**	**0.71**	**0.63**
CHO EDTA	**0.59**	**0.76**	**0.91**	0.40	_	_
AA MQ	**0.67**	**0.76**	**0.77**	**0.72**	**0.94**	**0.84**
AA EDTA	**0.81**	**0.90**	0.56	**0.56**	**0.82**	**0.83**

769

770

771 **Table 2.** Explanatory variables and EPS parameter notation

Explanatory variables		**EPS parameters**			
PAR	Photosynthetically Active Radiation (400-700 nm) during labeling	*Extracellular Polymeric Substances (EPS)*		*Amino Acids*	
Tsed	Sediment temperature	**EPS MQ**	Water-extractable EPS	**Asp**	aspartine
Photosynthetic Parameters		**EPS EDTA**	EDTA-extractable EPS	**Ser**	serine
ETRMax	Relative maximum reached electron transport rate	*Operational defined EPS fractions*		**Thr**	threonine
α	Light affinity coefficient in the light limited region of the rapid light curve	**CHO MQ**	Water-extractable carbohydrates	**Gly**	glycine
Ek	(minimum) Light saturation irradiance	**CHO EDTA**	EDTA-extractable carbohydrates	**Pro**	proline
Pigments		**AA MQ**	Water-extractable amino acids	**Ala**	alanine
β-CARO	β-Carotene	**AA EDTA**	EDTA-extractable amino acids	**Val**	valine
CLA	Chlorophyll a			**Met**	methionine
CLC	Chlorophyll c	**M**	Water-extractable	**Ile**	isoleucine
DIAD	Diadinoxanthine	**E**	EDTA-extractable	**Leu**	leucine
DIAT	Diatoxanthine	*Carbohydrates (CHO)*		**Tyr**	tyrosine
PHOR	Pheophorbide	**FUC**	fucose	**Lys**	lysine
FUCO	Pheophorbide	**RHA**	rhamnose	**His**	histine
Nutrients		**GAL**	galactose	**Phe**	phenylalanine
w-NH4	Water column ammonium	**GLC**	glucose	**Arg**	arginine
w-NO2	Water column nitrite	**XYL**	xylose		
w-NO3	Water column nitrate	**MAN**	mannose		
w-PO4	Water column phosphate				

w-Si	Water column silicate				
pw-NH4	Pore water ammonium				
pw-NO2	Pore water nitrite				
pw-NO3	Pore water nitrate				
pw-PO4	Pore water phosphate				
pw-Si	Pore water silicate				

Figures

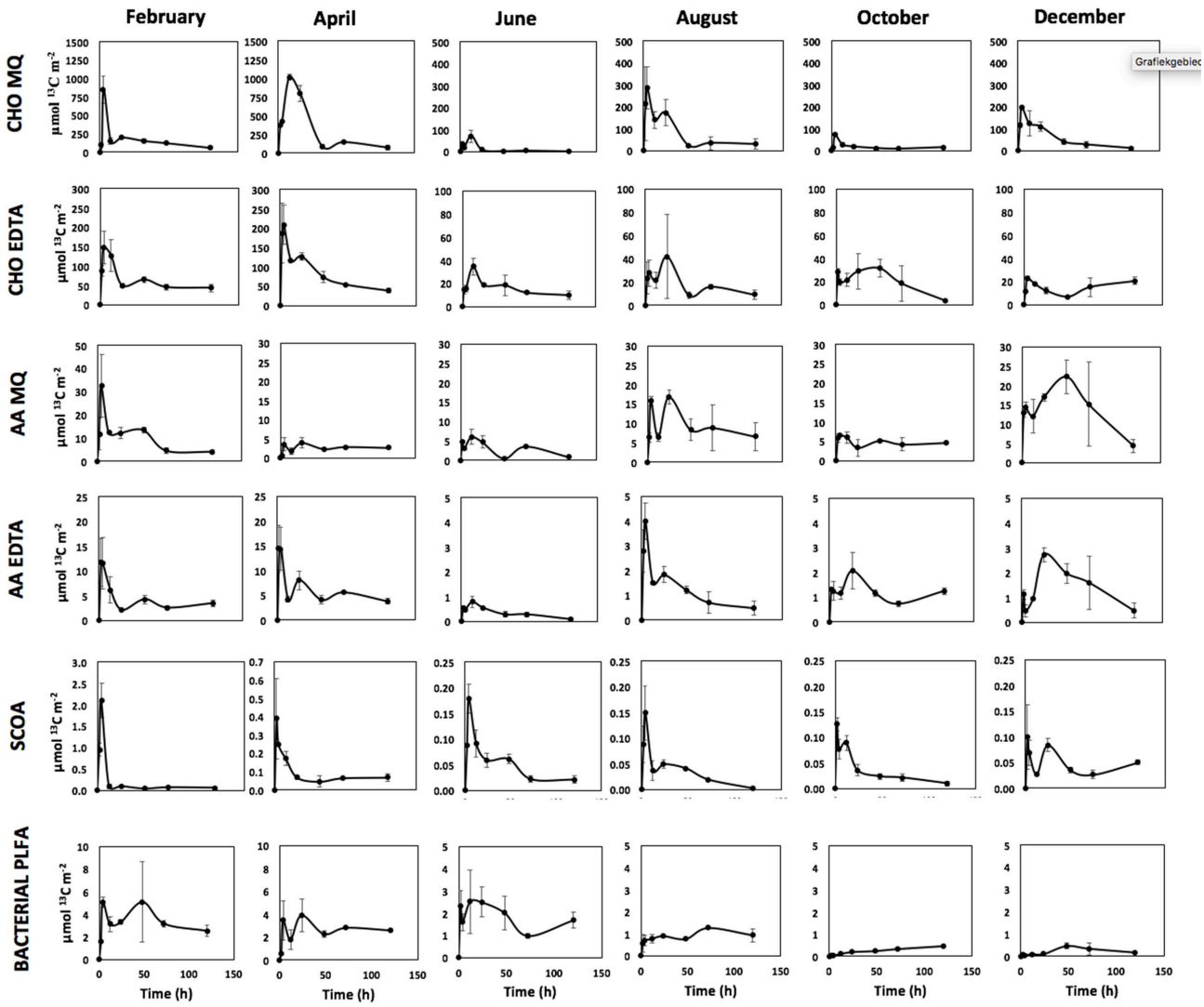

Fig. 1. An overview of ^{13}C label dynamics of excreted carbon pools (i.e. EPS and SCOA) and bacteria derived from heterotrophic consumption of these excreted carbon pools. In the two operational defined EPS extracts (i.e. EPS MQ and EPS EDTA) carbohydrates and amino acids were detectable. Note that the Y-axes of the panels for February and April differ from those of the other months (which are all the same). Also, the Y-axes of the panels for SCOA for February and April are not identical.

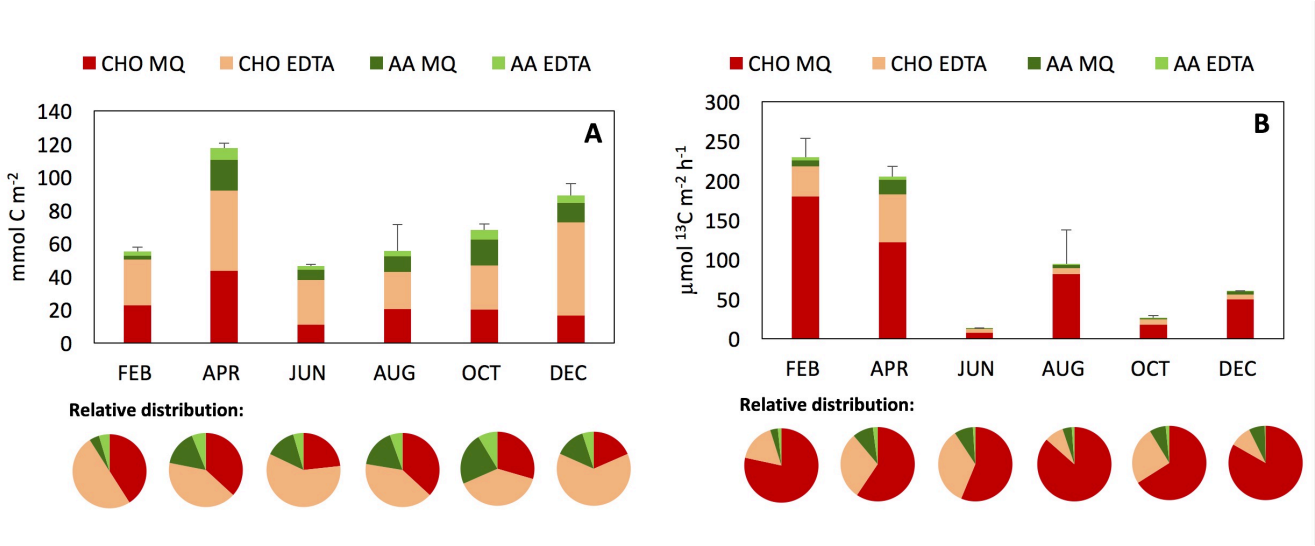

Fig. 2. Annual carbohydrate and amino acid (A) concentrations and (B) productions originated from EPS MQ and EPS EDTA.

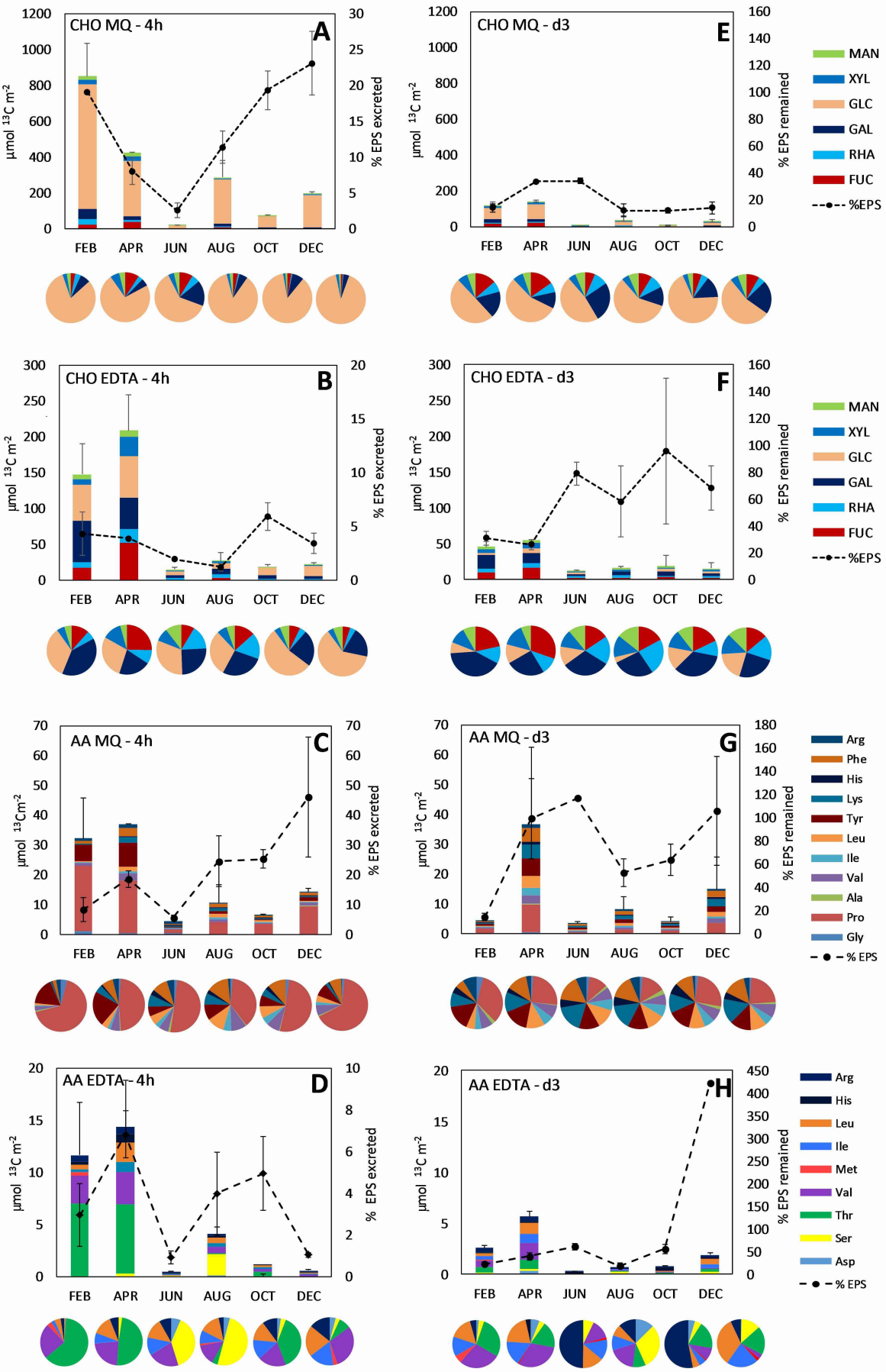
CHO MQ - 4h
A
CHO MQ - d3
E
CHO EDTA - 4h
B
CHO EDTA - d3
F
AA MQ - 4h
C
AA MQ - d3
G
AA EDTA - 4h
D
AA EDTA - d3
H
µmol ¹³C m⁻²
% EPS excreted
% EPS remained
FEB
APR
JUN
AUG
OCT
DEC
MAN
XYL
GLC
GAL
RHA
FUC
%EPS
Arg
Phe
His
Lys
Tyr
Leu
Ile
Val
Ala
Pro
Gly
% EPS
Met
Thr
Ser
Asp

Fig. 3. Annual carbohydrate monomers and amino acids ^{13}C label content of EPS MQ and EPS EDTA fractions. Details of ^{13}C label are presented for respectively 4 h (i.e. after initial ^{13}C label incorporation) and d3 (i.e. ^{13}C label distribution after 3 days). For panel A, B, C and D the dotted line represents the percentage of carbon initially fixed as respectively carbohydrate and amino acid and excreted as EPS. For panel E, F, G and H the dotted line represents the percentage of ^{13}C label remained in EPS after 3 days compared to the amount of ^{13}C label incorporated at t = 4h.

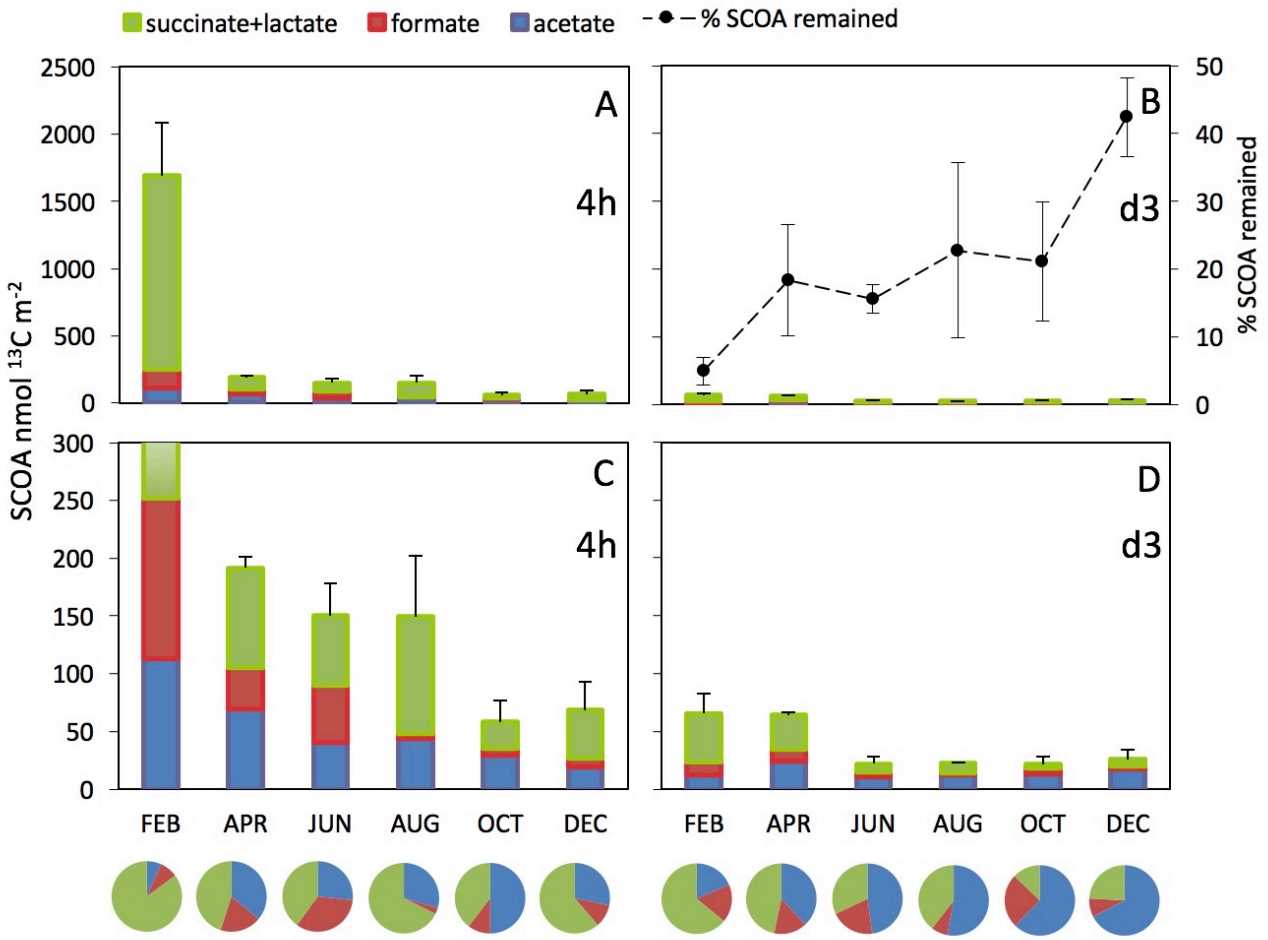

Fig. 4. Annual short chain organic acid (SCOA) details. Details are presented for respectively 4 h (i.e. after initial ^{13}C label incorporation) (panels A and C) and d3 (i.e. ^{13}C label distribution after 3 days) (panels B and D). The dotted line (panel B) represents the percentage of ^{13}C label remained in EPS after 3 days compared to the amount of ^{13}C label incorporated at t = 4h. Panels C and D represent enlargements of the panels A and B, respectively

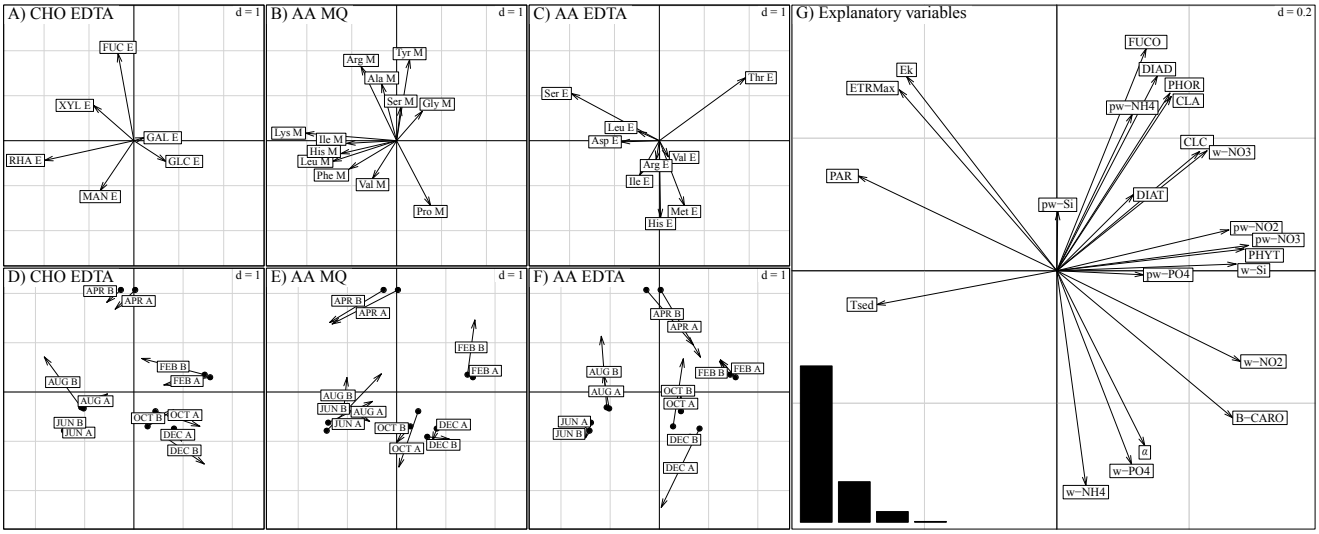

Fig. 5. Concordance Analysis of explanatory data and production details of both carbohydrates and amino acids originated from EPS MQ and EPS EDTA extracts. From A to C, variable interplay of the different EPS fractions. From D to E, positions of monthly samples; black dots, reference ordination of months induced by explanatory variables (G); arrow tips, positions induced by respective EPS fraction variables; arrow lengths indicate the lack of fitting. G, Explanatory variables; bar diagram, eigenvalues: axis 1 (horizontal), 75 %; axis 2 (vertical), 19 %. “d” indicates the grid scale. The notation of the various parameters is explained in table 2.

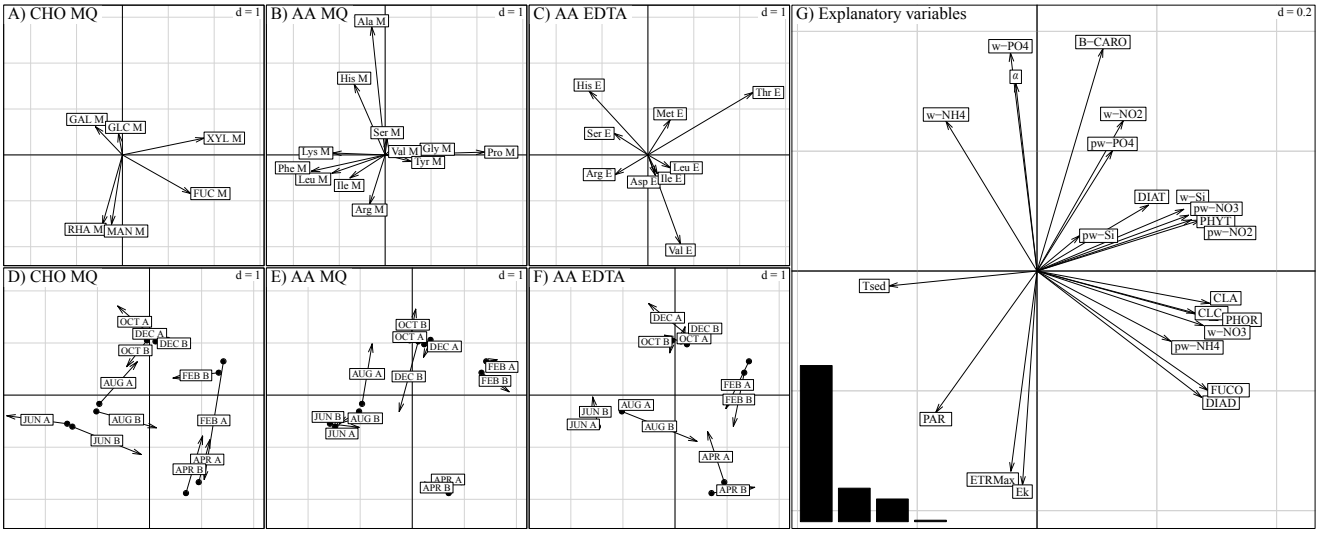

Fig. 6. Concordance Analysis of explanatory data and details of 13C label content of carbohydrates and amino acids originated from EPS MQ and EPS EDTA at t = 3 days. From A to C, variable interplays of the different EPS fractions. From D to E, positions of monthly samples; black dots, reference ordination of months induced by explanatory variables (G); arrow tips, positions induced by respective EPS fraction variables; arrow lengths indicate the lack of fitting. G, explanatory variables; bar diagram, eigenvalues: axis 1 (horizontal), 73 %; axis 2 (vertical), 16 %. “d” indicates the grid scale. The notation of the various parameters is explained in table 2.

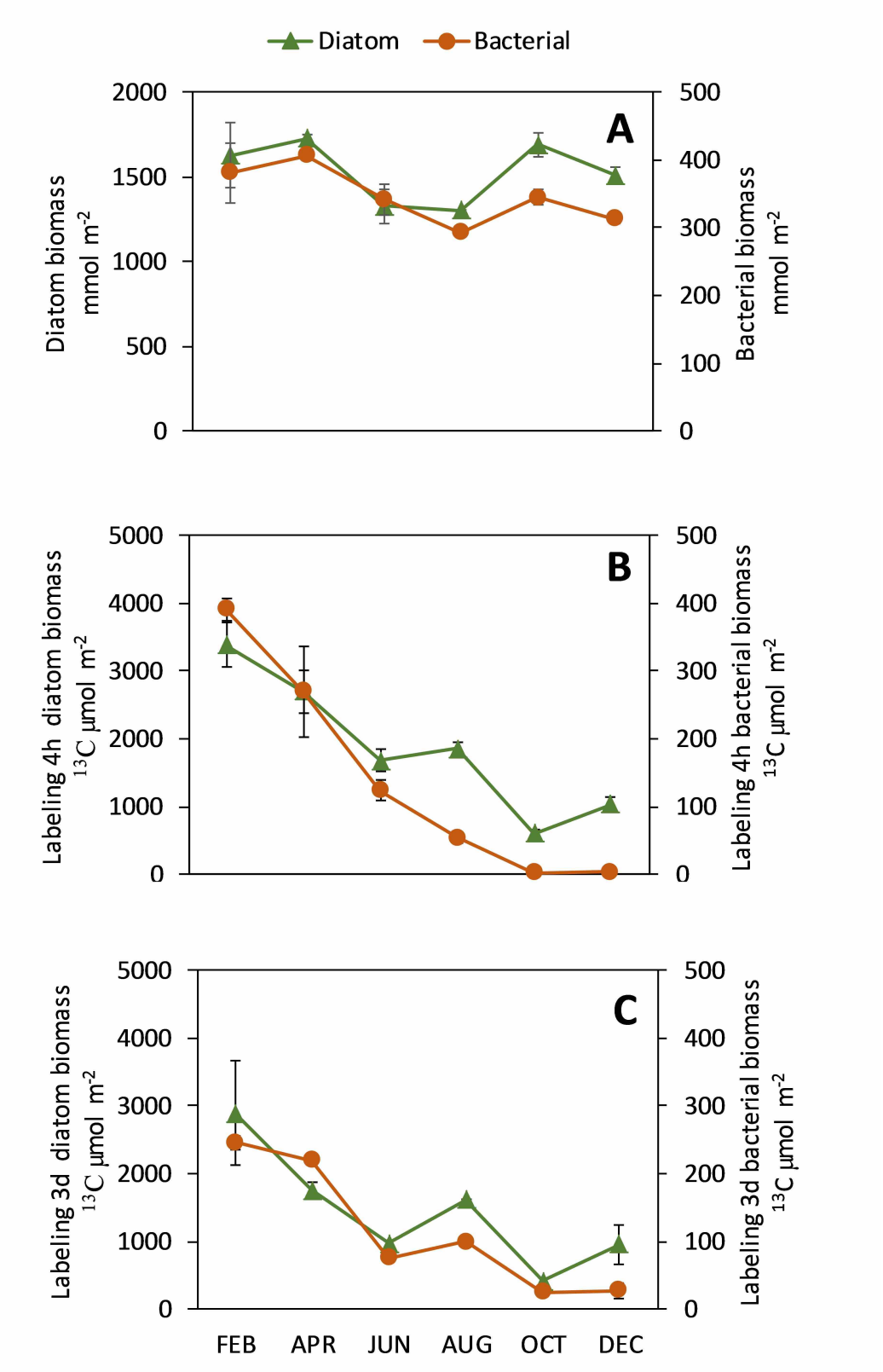

Fig. 7. Annual diatom and bacterial biomass (expressed in mmol C m^{-2}) (A), their ^{13}C labeling content at 4 h (expressed in µmol ^{13}C m^{-2}) (B) and their ^{13}C labeling content at day 3 (expressed in in µmol ^{13}C m^{-2}) (C) calculated from their respective specific phospholipid-derived fatty acids (PLFA).

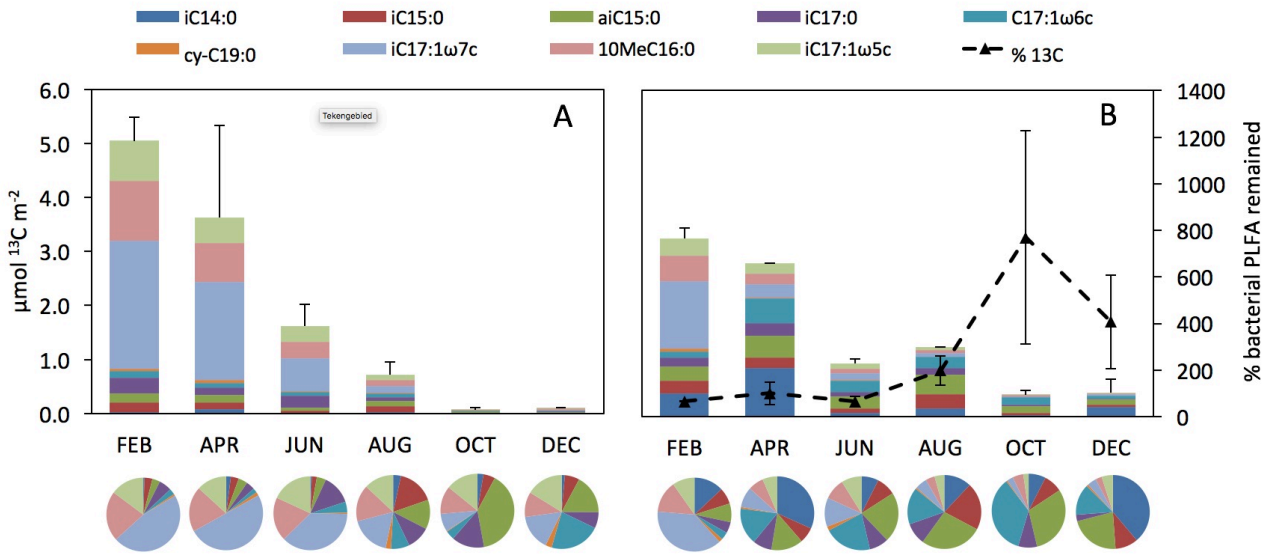

902

903

904 **Fig. 8.** Annual distribution of ^{13}C label in bacterial PLFA biomarkers. Details of ^{13}C label are
905 presented for 4 hours (i.e. after initial ^{13}C incorporation) (A) and after 3 days of ^{13}C label distribution
906 (B). The dotted line in panel B represents the percentage of ^{13}C label remaining in bacterial specific
907 PLFA after 3 days compared to the amount of ^{13}C label incorporated at t=4h.

908

909

Supplementary Table S1

Explanatory variables			Field		Pigments								PAM			Nutrients water						Nutrients pore water					
Sample	Sample Date	Low Tide	PAR	Tsed	β-CARO	CLA	CLC	DIAD	DIAT	PHOR	FUCO	PHYT	ETRMax	α	Ek	w-NH4	w-NO2	w-NO3	w-PO4	w-Si	w-N:P	pw-NH4	pw-NO2	pw-NO3	pw-PO4	pw-Si	pw-N:P
		h	µE m^{-2} s^{-1}	°C	mg m^{-2}								µE m^{-2} s^{-1}			µmol L^{-1}						µmol L^{-1}					
FEB A	21-Feb-11	11:40	1314	3.3	22	586	57	44	16	43	219	44	80	0.56	142	9	1.7	48	1.1	31	54	49	1.3	16	4	76	18
APR A	4-Apr-11	11:06	5277	8.7	16	608	59	41	21	52	226	17	257	0.41	621	3	0.8	38	0.5	10	86	106	0.8	7	4	72	17
JUN A	14-Jun-11	8:46	5891	15.6	14	365	45	18	10	15	124	8	182	0.55	334	10	0.9	6	0.8	6	23	24	0.2	1	1	39	40
AUG A	15-Aug-11	11:36	7492	19.7	18	465	42	18	18	28	139	8	255	0.58	437	7	0.9	4	1.2	9	10	22	0.5	1	3	91	26
OCT A	10-Oct-11	9:24	2484	12.5	26	555	50	20	23	32	159	14	88	0.60	147	8	1.4	10	1.4	10	14	67	0.5	6	15	119	8
DEC A	12-Dec-11	10:25	1392	6.4	27	460	54	23	18	30	139	30	92	0.66	139	9	1.3	20	1.3	20	22	36	0.8	12	3	44	16
FEB B	21-Feb-11	11:40	1314	4.1	23	610	60	47	16	44	227	47	153	0.74	205	9	1.7	48	1.1	31	54	45	0.9	18	2	40	18
APR B	4-Apr-11	11:06	5277	9.7	14	577	54	38	20	53	212	15	299	0.39	776	3	0.8	38	0.5	10	86	101	0.5	7	3	79	24
JUN B	14-Jun-11	8:46	5891	16.4	14	379	45	18	12	17	129	8	198	0.55	360	10	0.9	6	0.8	6	23	29	0.2	1	1	40	36
AUG B	15-Aug-11	11:36	7492	21.2	15	456	42	18	15	24	149	10	230	0.58	395	7	0.9	4	1.2	9	10	31	0.4	1	4	78	21
OCT B	10-Oct-11	9:24	2484	12.8	25	512	46	17	21	30	149	14	82	0.62	132	8	1.4	10	1.4	10	14	48	0.5	7	9	101	12
DEC B	12-Dec-11	10:25	1392	7.0	26	423	49	21	14	27	133	26	99	0.66	149	9	1.3	20	1.3	20	22	39	0.9	10	3	43	14

Supplementary Table S2

Production variables			*Carbohydrates*												*Amino acids*																				
			CHO MQ						CHO EDTA						AA MQ												AA EDTA								
Sample	Date	Low Tide	FUC M	RHA M	GAL M	GLC M	XYL M	MAN M	FUC E	RHA E	GAL E	GLC E	XYL E	MAN E	Ser M	Gly M	Pro M	Ala M	Val M	Ile M	Leu M	Tyr M	Lys M	His M	Phe M	Arg M	Asp E	Ser E	Thr E	Val E	Met E	Ile E	Leu E	His E	Arg E
		h	µmol ^{13}C m^{-2} h^{-1}						µmol ^{13}C m^{-2} h^{-1}						µmol ^{13}C m^{-2} h^{-1}												µmol ^{13}C m^{-2} h^{-1}								
FEB A	21-02-11	11:40	3.9	2.1	11.9	185	5.3	4.8	3.2	1.7	10.0	13.0	1.7	1.5	0.03	0.22	4.00	0.03	0.28	0.05	0.07	0.62	0.05	0.04	0.17	0.09	0.02	0.02	1.78	0.63	0.10	0.06	0.10	0.05	0.23
APR A	04-04-11	11:06	10.9	3.8	6.2	89	6.3	3.4	16.9	6.2	18.7	24.8	8.5	3.1	0.16	0.24	2.61	0.38	1.02	0.97	1.64	2.00	2.15	0.55	2.16	0.77	0.01	0.10	3.08	0.92	0.02	0.33	0.65	0.38	0.21
JUN A	14-06-11	8:46	0.6	0.3	1.4	5	0.3	0.2	0.3	0.5	1.1	1.3	0.3	0.4		0.02	0.52	0.02	0.06	0.02	0.05	0.05	0.08	0.03	0.08	0.06	0.01	0.04	0.00	0.03	0.00	0.02	0.03	0.01	0.03
AUG A	15-08-11	11:36	2.6	0.8	4.8	108	2.3	2.0	1.2	1.6	2.7	4.8	0.7	0.6	0.04	0.06	1.50	0.01	0.43	0.23	0.47	0.42	0.29	0.10	0.56	0.03	0.03	0.51	0.03	0.15	0.00	0.08	0.10	0.09	0.02
OCT A	10-10-11	9:24	0.5	0.1	1.5	16	0.3	0.2	0.5	0.3	1.8	4.3	0.3	0.5	0.02	0.04	1.05	0.00	0.17	0.10	0.13	0.08	0.07	0.04	0.21	0.00	0.01	0.01	0.11	0.06	0.00	0.03	0.03	0.07	0.01
DEC A	12-12-11	10:25	0.6	0.2	2.0	46	0.9	0.6	0.4	0.3	1.2	3.5	0.2	0.4	0.02	0.07	2.81	0.03	0.29	0.09	0.19	0.26	0.07	0.04	0.40	0.02	0.00	0.01	0.01	0.07	0.01	0.03	0.03	0.06	0.02
FEB B	21-02-11	11:40	7.9	11.3	13.2	104	5.1	4.6	6.3	3.0	19.9	11.4	2.6	2.4	0.05	0.39	5.99	0.07	0.23	0.07	0.13	1.94	0.09	0.04	0.29	0.39	0.01	0.03	2.36	0.86	0.09	0.09	0.16	0.09	0.38
APR B	04-04-11	11:06	10.5	3.5	5.9	92	7.4	4.7	10.4	3.5	9.0	13.0	5.0	1.9	0.20	0.33	3.60	0.49	1.54	1.47	2.68	3.34	3.41	0.87	3.26	1.22	0.01	0.07	1.28	0.84	0.01	0.18	0.31	0.10	0.16
JUN B	14-06-11	8:46	0.3	0.3	0.8	5	0.2	0.2	0.5	0.8	1.4	1.7	0.5	0.6		0.01	0.57	0.01	0.07	0.04	0.08	0.08	0.08	0.04	0.13	0.05	0.01	0.04	0.00	0.02	0.00	0.01	0.01	0.00	0.02
AUG B	15-08-11	11:36	2.3	0.5	3.6	34	1.0	1.1	0.7	0.7	1.2	0.7	0.4	0.4	0.04	0.05	0.75	0.01	0.35	0.24	0.44	0.50	0.38	0.10	0.48	0.07	0.04	0.55	0.05	0.15	0.00	0.11	0.19	0.03	0.05
OCT B	10-10-11	9:24	0.5	0.1	1.4	13	0.2	0.2	0.4	0.3	1.5	2.8	0.3	0.4	0.01	0.04	0.94	0.01	0.16	0.08	0.14	0.15	0.07	0.04	0.23	0.00	0.01	0.01	0.21	0.09	0.00	0.06	0.06	0.05	0.00
DEC B	12-12-11	10:25	0.8	0.3	2.3	44	0.9	0.7	0.2	0.2	1.0	3.3	0.2	0.3	0.02	0.06	2.67	0.00	0.29	0.07	0.14	0.35	0.05	0.02	0.33	0.01	0.00	0.00	0.03	0.07	0.00	0.03	0.04	0.02	0.04

Supplementary Table S3

Day 3 variables		*Carbohydrates*												*Amino acids*																				
		CHO MQ						CHO EDTA						AA MQ														AA EDTA								
Sample	Date	FUC M	RHA M	GAL M	GLC M	XYL M	MAN M	FUC E	RHA E	GAL E	GLC E	XYL E	MAN E	Ser M	Gly M	Pro M	Ala M	Val M	Ile M	Leu M	Tyr M	Lys M	His M	Phe M	Arg M	Asp E	Ser E	Thr E	Val E	Met E	Ile E	Leu E	His E	Arg E
		µmol ^{13}C m^{-2}						µmol ^{13}C m^{-2}						µmol ^{13}C m^{-2}												µmol ^{13}C m^{-2}								
FEB A	24-02-11	19.6	10.2	19.2	44.1	8.0	6.4	10.8	6.0	21.9	3.8	5.7	4.4	0.10	0.25	1.74	0.14	0.43	0.24	0.29	0.93	0.43	0.25	0.35	0.50	0.07	0.09	0.66	0.51	0.18	0.35	0.35	0.11	0.53
APR A	07-04-11	22.1	8.3	14.6	76.0	9.7	7.7	17.2	6.1	13.8	6.6	8.1	3.6	0.17	0.21	3.12	0.05	0.90	0.77	1.03	1.38	1.31	0.37	1.43	0.46	0.06	0.28	0.87	1.58	0.05	0.95	1.13	0.37	0.58
JUN A	17-06-11	0.4	0.6	1.9	3.5	0.0	0.3	2.1	2.5	4.0	1.6	1.5	1.5		0.06	0.47	0.03	0.24	0.23	0.38	0.25	0.62	0.18	0.43	0.21	0.00	0.03	0.00	0.05	0.00	0.03	0.03	0.17	0.07
AUG A	18-08-11	1.8	1.4	2.7	21.4	1.1	1.3	2.1	3.3	4.3	0.6	1.9	1.9	0.11	0.19	1.99	0.40	0.85	0.95	1.30	1.63	1.87	0.72	1.63	0.74	0.14	0.29	0.06	0.16	0.04	0.09	0.07	0.14	0.17
OCT A	13-10-11	0.6	0.5	1.6	8.4	0.4	0.3	0.6	0.4	0.9	0.7	0.3	0.3	0.07	0.10	1.53	0.08	0.44	0.36	0.53	0.85	0.70	0.47	0.58	0.11	0.03	0.03	0.14	0.06	0.01	0.03	0.03	0.46	0.04
DEC A	15-12-11	0.7	0.3	1.3	4.9	0.3	0.3	3.5	4.0	6.0	4.4	3.1	2.6	0.05	0.07	1.09	0.08	0.38	0.19	0.40	0.54	0.55	0.20	0.56	0.10	0.00	0.26	0.05	-0.02	0.04	0.10	0.14	0.06	0.06
FEB B	24-02-11	14.1	7.0	23.7	78.4	8.3	7.0	9.0	4.2	15.7	2.7	4.1	3.1	0.06	0.12	1.31	0.06	0.23	0.14	0.20	0.52	0.37	0.14	0.16	0.29	0.00	0.07	0.57	0.71	0.04	0.23	0.33	0.07	0.24
APR B	07-04-11	21.5	10.0	15.9	82.9	10.0	7.4	15.8	5.9	13.7	7.0	7.6	3.5	0.61	0.79	15.46	0.27	4.94	3.89	7.50	10.12	7.76	1.79	7.99	1.85	0.56	0.12	1.00	1.57	0.03	0.81	0.99	0.00	0.39
JUN B	17-06-11	0.5	0.6	1.4	2.5	0.3	0.4	1.7	2.0	3.5	1.5	1.2	1.2		0.07	0.36	0.06	0.29	0.26	0.49	0.67	0.61	0.19	0.71	0.25	0.00	0.00	0.00	0.00	0.01	0.03	0.03	0.03	0.07
AUG B	18-08-11	1.4	1.3	2.5	10.9	1.1	1.3	3.3	4.2	4.3	0.6	2.7	2.7	0.05	0.08	0.47	0.06	0.29	0.27	0.52	0.45	0.67	0.24	0.80	0.30	0.01	0.08	0.05	0.06	-0.03	0.03	0.03	0.00	0.06
OCT B	13-10-11	0.4	0.3	0.9	3.9	0.2	0.3	6.0	3.3	11.8	4.9	4.0	3.6	0.06	0.05	0.60	0.08	0.20	0.17	0.29	0.32	0.28	0.10	0.34	0.04	0.03	0.03	0.11	0.06	0.00	0.04	0.03	0.24	0.04
DEC B	15-12-11	1.3	0.8	2.4	8.2	0.8	0.4	0.8	1.0	1.6	1.6	1.1	1.2	0.30	0.23	5.72	0.32	2.14	1.48	2.59	3.39	4.07	1.11	3.60	1.00	0.01	0.17	0.59	-0.09	0.02	0.62	0.97	0.18	0.43